

A cooperative and specific DNA-binding mode of HIV-1 integrase depends on the nature of the metallic cofactor and involves the zinc-containing N-terminal domain

Kevin Carayon, Hervé Leh, Etienne Henry, Françoise Simon, Jean-François Mouscadet and Eric Deprez*

LBPA, CNRS, Ecole Normale Supérieure de Cachan, 61 av. du Président Wilson, 94235 Cachan, France

Received July 23, 2009; Revised and Accepted February 2, 2010

ABSTRACT

HIV-1 integrase catalyzes the insertion of the viral genome into chromosomal DNA. We characterized the structural determinants of the 3'-processing reaction specificity—the first reaction of the integration process—at the DNA-binding level. We found that the integrase N-terminal domain, containing a pseudo zinc-finger motif, plays a key role, at least indirectly, in the formation of specific integrase–DNA contacts. This motif mediates a cooperative DNA binding of integrase that occurs only with the cognate/viral DNA sequence and the physiologically relevant Mg^{2+} cofactor. The DNA-binding was essentially non-cooperative with Mn^{2+} or using non-specific/random sequences, regardless of the metallic cofactor. 2,2'-Dithiobisbenzamide-1 induced zinc ejection from integrase by covalently targeting the zinc-finger motif, and significantly decreased the Hill coefficient of the Mg^{2+} -mediated integrase–DNA interaction, without affecting the overall affinity. Concomitantly, 2,2'-dithiobisbenzamide-1 severely impaired 3'-processing ($IC_{50} = 11–15\text{ nM}$), suggesting that zinc ejection primarily perturbs the nature of the active integrase oligomer. A less specific and weaker catalytic effect of 2,2'-dithiobisbenzamide-1 is mediated by Cys 56 in the catalytic core and, notably, accounts for the weaker inhibition of the non-cooperative Mn^{2+} -dependent 3'-processing. Our data show that the cooperative DNA-binding mode is strongly related to the sequence-specific DNA-binding, and depends on the simultaneous presence of the Mg^{2+} cofactor and the zinc effector.

Integration of HIV-1 DNA into the host genome ensures stable maintenance of the viral genome in the host organism and, therefore, is a key process in the virus life cycle. Integrase (IN) is responsible for two distinct, consecutive catalytic steps in the integration process (1). The first of these two reactions is 3'-processing, which corresponds to the specific cleavage of two nucleotides from the 3'-ends of the linear viral DNA. The hydroxyl groups of newly recessed 3'-ends are then used in the second reaction—strand transfer—for the covalent joining of viral and cellular (or target) DNAs, resulting in full-site integration. For both reactions, IN functions as a multimer, most likely a dimer for 3'-processing and a tetramer (dimer of a dimer) for concerted integration (2–7). Two other reactions occur *in vitro*, a disintegration reaction that represents, in first approximation, the reversal of the half-site integration process (8) and a specific internal cleavage occurring on a symmetrical DNA site (9). All reactions require a metallic cofactor, Mg^{2+} or Mn^{2+} , and, except for disintegration (10,11), all reactions require the full-length IN. There are several experimental evidences to suggest that Mg^{2+} is more physiologically relevant as a cofactor, particularly because Mg^{2+} -dependent catalysis exhibits weaker non-specific endonucleolytic cleavage and the tolerance of sequence variation at the ends of the viral DNA is much greater in the presence of Mn^{2+} than in the presence of Mg^{2+} (12–15).

The emergence of viral strains resistant against available drugs and the dynamic nature of the HIV-1 genome support a continued effort towards the discovery and characterization of novel targets and anti-viral drugs. Due to its central role in the HIV-1 life cycle, IN represents a promising therapeutic target. In the past, *in vitro* IN assays were extensively used to find IN inhibitors (16). Current inhibitors can be separated into two main classes, depending on their mechanisms of action: (i) Compounds that competitively prevent the DNA binding of IN to the

*To whom correspondence should be addressed. Tel: +33 147 40 23 94; Fax: +33 147 40 76 71; Email: deprez@lbpa.ens-cachan.fr

viral DNA. These compounds are mainly directed against the 3'-processing reaction as they bind to the donor site within the catalytic site—i.e. the 'specific' DNA-binding site for the viral DNA. This group is referred to as 'integrase DNA-binding inhibitors' (INBI) and includes styrylquinoline compounds (17,18). (ii) The second class includes compounds that cannot bind to the DNA-free IN. They bind to the pre-formed IN–viral DNA complex. These compounds preferentially inhibit strand transfer over the 3'-processing reaction [this family of compounds is referred to as 'integrase strand transfer inhibitors' (INSTI)], probably by displacing the viral DNA end from the active site (7,19–21). It is not clear whether this mechanism alone accounts for the inhibitory properties of INSTIs or whether these compounds also prevent the binding of the target DNA to the acceptor site—i.e. the 'non-specific' DNA binding site. INSTI compounds have generally good *ex vivo* activity against HIV replication, probably due to their ability to inhibit pre-assembled viral DNA/IN complexes. Raltegravir which is currently used in clinical treatment of HIV-1 belongs to this class. For both anti-IN classes, resistance mutations were identified (17,20,22,23). Difficulties in deeply understanding their mechanisms of action are closely related to the absence of structural data that clearly delineate the donor and the acceptor DNA binding sites in the active site. Although structural information is now available regarding the IN–viral DNA interaction, based on the recent crystal structure of the full-length primate foamy virus (PFV-1) IN in complex with its cognate processed viral DNA, the target DNA binding mode and the precise location of the acceptor site remains open to debate (7). Moreover, it is a difficult task to experimentally discriminate between the two DNA binding sites and no significant or only modest difference can be evidenced *in vitro* (depending on the method used for monitoring IN–DNA interactions) between the HIV-1 IN binding to the cognate viral DNA sequence and a non-specific random sequence in terms of overall affinity, suggesting that the specific and the non-specific DNA-binding modes display similar binding free energies (5,24). The basis of DNA binding specificity remains essentially unknown.

HIV-1 IN (288 amino acids) contains three functional domains. The central domain or catalytic core domain (IN^{50–213} or CC) contains the catalytic triad (DDE) that coordinates one or two metallic cofactors [probably a pair coordinated by three carboxylate groups of the triad, based on the X-ray structure of the PFV-1 IN (7)] and is essential for enzymatic activity; this domain alone can perform the disintegration reaction (10,11). This domain is flanked by the N-terminal (IN^{1–49}) and the C-terminal (IN^{214–288}) domains. The C-terminal domain is involved in IN–DNA contacts, together with the CC domain (25,26). The N-terminal domain contains a conserved non-conventional HHCC motif that binds zinc to ensure proper domain folding and promotes IN multimerization (27–29). It is worth noting that the integrity of the HHCC motif is crucial in the stringent Mg²⁺-context but appears dispensable under the less stringent Mn²⁺ condition (30), suggesting, at least, an indirect role of the zinc-binding

domain in the establishment of specific and physiologically relevant IN–DNA complexes. In the structure of the PFV-1 IN–viral DNA complex, the N-terminal domain is also involved in the interaction with DNA (7).

In this article, we found that IN binds cooperatively to the cognate viral DNA sequence only in the presence of Mg²⁺. The presence of Mn²⁺ or, most importantly, the use of non-specific random sequences, regardless of the metallic cofactor, dramatically reduced the Hill coefficient. This finding suggests that the cooperative DNA-binding mode of IN is strongly related to the formation of specific IN–DNA contacts. To gain deeper insight into the role of the zinc-binding domain in the cooperative/multimerization process, in relationship with the establishment of specific protein–DNA contacts, we studied the effect of DIBA-1 (2,2'-dithiobisbenzamide-1) (Figure 1A) on IN activity. This compound is a zinc ejector affecting many proteins containing zinc fingers, including HIV-1 nucleocapsid or estrogen receptor (31–34). Here, we found that DIBA-1 induced zinc ejection from the IN N-terminal domain by covalently targeting the HHCC motif. In the presence of Mg²⁺, DIBA-1 did not affect significantly the overall affinity of IN for the DNA substrate but dramatically reduced the Hill coefficient. Concomitantly, DIBA-1 strongly inhibited the catalytic step, with IC₅₀ values against the 3'-processing reaction of 11–15 nM. Interestingly, we found a secondary DIBA-1 binding site in the catalytic core (involving residue Cys 56), suggesting a second mechanism of action of DIBA-1, independent of zinc ejection. The prevalence of the two distinct mechanisms was dependent on the cofactor context, with the second one accounting for the weaker DIBA-1 inhibitory effect under Mn²⁺ conditions (IC₅₀ = 115–126 nM). DIBA-1 behaves as a non-competitive/catalytic inhibitor that did not disturb the fractional saturation of DNA sites, regardless of the mechanism considered.

Altogether, our results show that, although it is a difficult task to discriminate between the specific viral sequence and a non-specific random sequence in terms of overall affinity, these sequences lead to distinct DNA-binding properties in terms of cooperativity. Moreover, our results highlight that the Mg²⁺-dependent catalytic activity of IN is strongly sensitive to the loss of cooperative DNA binding. Such a cooperative DNA-binding mode accounts for specific activity and requires: (i) the cognate viral DNA sequence, (ii) Mg²⁺ as a catalytic cofactor and (iii) zinc which can be considered as a positive allosteric effector. Development of non-competitive compounds acting on the N-terminal domain may be of interest for anti-IN pharmacology.

MATERIALS AND METHODS

Oligonucleotides and DIBA-1

The oligonucleotides, U5A (5'-GTG TGG AAA ATC TCT AGC AGT), and its complementary strand, U5B (5'-ACT GCT AGA GAT TTT CCA CAC), mimicking the HIV-1 DNA U5 extremity, were used for the 3'-processing assay. For the DNA-binding assay, U5A

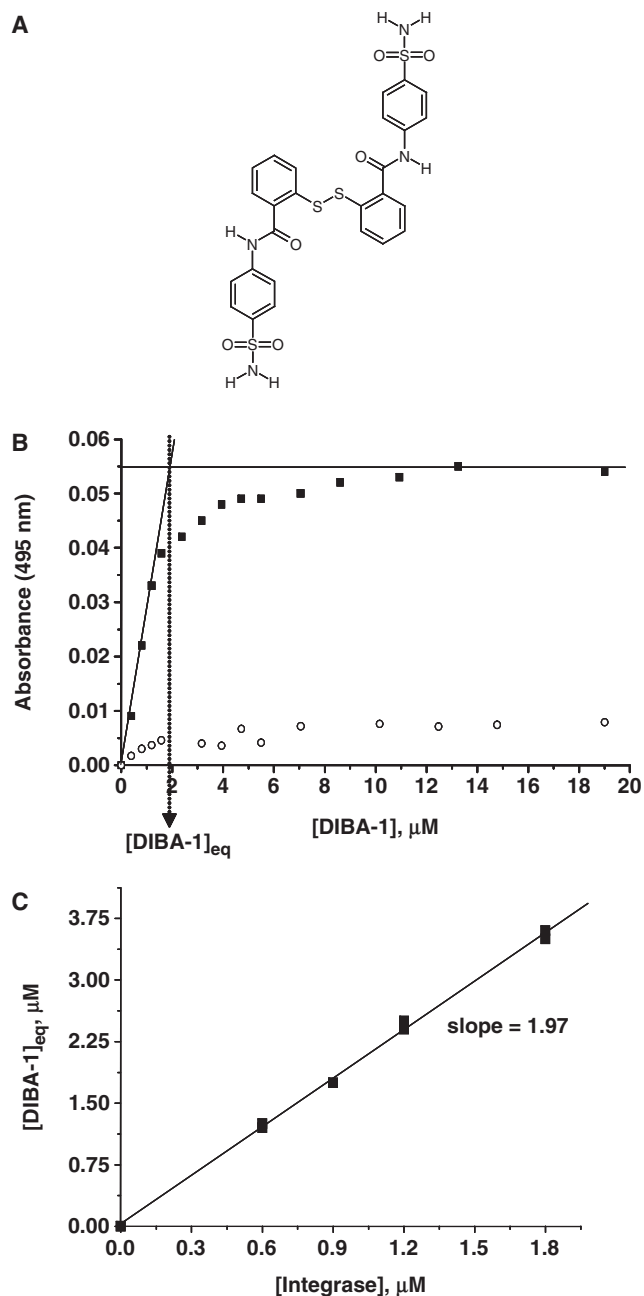


Figure 1. DIBA-1 induces the ejection of zinc from IN. (A) Structure of 2,2'-dithiobisbenzamide-1 (DIBA-1) (MW, 614 Da). (B) Ejection of zinc was measured by optical absorbance at 495 nm using a sample containing full-length IN (1 μM) and PAR (10^{-4} M) in a Tris buffer (20 mM pH 7.0) containing 15% DMSO (v/v) in the absence of reducing agent (black squares) or in the presence of 4 mM β-mercaptoethanol (white circles). The concentration of DIBA-1 for complete zinc release— $[DIBA-1]_{eq}$ —was estimated graphically. This value was determined as a function of the initial concentration of IN (C). The slope of the straight line indicates that the zinc ejection coincides with the reaction of two DIBA-1 molecules per IN protomer.

was fluorescein-labeled on the 3'-end to produce U5A-3'-F. The two random sequences used for DNA binding were RAND1A (5'-ACA TAA TCT AAA ATA ATT GCC-3'-F) and RAND2A (5'-ACC TAT GCG CCG CTA GAT TCC-3'-F) and their complementary strands,

RAND1B and RAND2B, respectively. Disintegration activity was measured using a dumbbell substrate D (5'-TGC TAG TTC TAG CAG GCC CTT GGG CCG GCG CTT GCG CC) as previously described (11). One- and two-domain truncation constructs (ΔN , ΔC and CC) were generated by PCR using the following oligonucleotides: $\Delta NPCR$ 5'-CAT ATG CAT GGA CAA GTA GAC TG; T7Term 5'-TGC TAG TTA TTG CTC AGC GG; $\Delta CPCR$ 5'-GGA TCC CTA TAA TTC TTT AGT TTG TA; T7Prom 5'-TAA TAC GAC TCA CTA TAG G. All oligonucleotides were purchased from Eurogentec (Liege, Belgium) and further purified by electrophoresis on a 15% denaturing acrylamide/urea gel. DIBA-1 was a generous gift from Sanofi-aventis (France).

Production and purification of full-length and truncated IN

All proteins (except IN¹⁻²¹³) contain the C280S mutation to avoid intermolecular disulfide bridges that promote covalent multimers in the absence of reducing agents (35). C56S, C65S and C56S-C65S mutations were introduced (in the context of the C280S mutant) into a pET-15b-IN plasmid encoding His-tagged HIV-1 IN (18). Site-directed mutagenesis was done using Stratagene's Quickchange[®] II Site-directed Mutagenesis kit and verified by DNA sequencing. One- and two-domain truncation constructs, IN⁵⁰⁻²⁸⁸ (or ΔN), IN¹⁻²¹³ (or ΔC) and IN⁵⁰⁻²¹³ (or CC) were generated from the full-length C280S IN by PCR. Primers ($\Delta NPCR$ and T7Term for ΔN ; T7Prom and $\Delta CPCR$ for ΔC ; $\Delta NPCR$ and $\Delta CPCR$ for CC) were designed to generate DNA fragments containing an NdeI site at the 5'-termini and a stop codon flanked by a BamHI site at the 3'-termini. The resulting PCR fragments were first introduced in pGEM[®]-T easy vector (Promega). The sequences encoding for the different truncated proteins were then cloned into pET-15b plasmid after a double NdeI-BamHI digestion. The different His-tagged proteins were overexpressed in *Escherichia coli* BL21-codonplus[®] (DE3+) (Stratagene[®]) and purified as previously described (18), with modifications. Briefly, bacterial cultures were incubated at 37°C and protein expression was induced by IPTG (final concentration, 0.25 mM) at $OD_{600nm} \approx 0.7$. The temperature was then lowered to 25°C and cultures were further incubated for 5 h. Purification was performed using Ni-NTA beads (Qiagen). The reducing agent (β-mercaptoethanol) was removed during washing/elution steps and subsequent dialysis. All purification buffers were supplemented with 50 μM ZnSO₄ except for proteins used for quantification of Zn²⁺ ejection by spectroscopy (see below), in order to reduce the background signal due to free Zn²⁺. Proteins were aliquoted, rapidly frozen in liquid nitrogen, and stored at -80°C. The full-length wild-type IN (used for comparison with the C280S mutant in the first section of Results, Table 1) was purified as previously described (18) without any modification.

Table 1. Hill coefficients characterizing the binding of HIV-1 full-length IN to different DNA sequences^a

Metallic cofactor ^b	Hill coefficient		
	U5A/ U5B	RAND1A/ RAND1B	RAND2A/ RAND2B
Mg ²⁺	1.97 ± 0.10	1.17 ± 0.06	1.20 ± 0.07
Mn ²⁺	1.29 ± 0.09	0.90 ± 0.06	0.92 ± 0.10

^aSee 'Materials and Methods' section for details.^b10 mM.

3'-Processing and disintegration reactions

Determination of IC₅₀ values. For activity assays, 100 pmol of either U5A (3'-processing substrate) or D (disintegration substrate) were radiolabelled using T4 polynucleotide kinase and 50 μCi of [γ -³²P]ATP (3000 Ci/mmol). The T4 kinase was then heat inactivated. NaCl was added to U5A and D (final concentration, 100 mM). The complementary strand U5B was added to U5A. The mixtures were incubated at 85°C for 5 min and allowed to anneal by slowly cooling to room temperature. Unincorporated nucleotides were removed by filtration through a Sephadex G-25 column (GE Healthcare). The 3'-processing or disintegration reactions were performed using 1 nM of either U5A/U5B or D DNA, respectively, in a buffer containing 20 mM Tris pH 7.0, 15% DMSO (v/v), 50 mM NaCl, 10 mM Mg²⁺ or Mn²⁺, full-length IN or truncated proteins (concentrations are indicated in the figure legends), and increasing amounts of DIBA-1. To assess the influence of the order of addition of reagents on the IC₅₀ values, three different protocols were tested: (i) DIBA-1 was preincubated with the metallic cofactor (for 15 min at 25°C) before addition of IN and DNA (protocol 1); (ii) DIBA-1 was preincubated with IN (for 15 min at 25°C) before addition of the metallic cofactor and DNA (protocol 2); (iii) IN was preincubated with the metallic cofactor (for 15 min at 25°C) before addition of DIBA-1 and DNA (protocol 3). Reaction mixtures were further incubated for 3 h at 37°C, and then stopped with 80 μl of a buffer containing 6 mM EDTA, 0.125 mg/ml glycogene, 400 mM NaOAc, followed by a phenol-chloroform extraction. DNA fragments were precipitated with ethanol, dissolved in a loading buffer containing 20 mM EDTA, 80% formamide, 0.05% bromophenol blue, 0.05% xylene cyanol and subjected to electrophoresis on an 12% denaturing acrylamide/urea gel. Gels were analyzed on a STORM 840TM PhosphorImager (Molecular Dynamics, Sunnyvale, CA, USA) and quantified using Image QuanTTM 4.1 software. The midpoint (IC₅₀) of the inhibition curve represents the drug concentration giving 50% inhibition.

DNA-binding assay and time-resolved fluorescence anisotropy

The interaction between IN and the 21-mer double-stranded, fluorescein-labeled oligonucleotide (U5A/U5B, RAND1A/RAND1B or RAND2A/RAND2B) was detected by steady-state fluorescence

anisotropy using a Beacon 2000 instrument (PanVera, Madison, WI, USA) (3,18,36). The double-stranded DNA was obtained by mixing equimolar amounts of complementary strands (B and A-3'-F) in a 20 mM Tris-HCl buffer (pH 7.0) containing 100 mM NaCl. The mixture was heated to 85°C for 5 min and allowed to anneal by slowly cooling to room temperature. To determine the apparent K_d -value ($K_{d,app}$), fluorescein-labeled DNA (1 nM) was incubated with increasing concentrations of IN (full-length or truncated proteins) in a 20 mM Tris buffer (pH 7.0) containing 15% DMSO (v/v), 50 mM NaCl and 10 mM MnCl₂ or MgCl₂ for 20 min at 25°C, and the steady-state anisotropy (r) was then recorded. In the presence of DIBA-1, titration experiments were performed with a constant DIBA-1:IN ratio (from 1:1 to 3:1). The fractional saturation Y was calculated as $(r - r_{free}) / (r_{bound} - r_{free})$, where r_{bound} and r_{free} represent the bound and free DNA anisotropy, respectively. The Hill number, \tilde{n} , was calculated by directly fitting the titration curve using the Hill function in Origin 6.0 software. $K_{d,app}$ or IN₅₀ represents the concentration of IN required to titrate the DNA to half saturation. Hydrodynamic characterization of the IN-DNA complexes (using fluorescein-labeled DNA U5A/U5B or RAND1A/RAND1B), via the determination of the rotational correlation times, was performed by time-resolved fluorescence anisotropy as previously described (3), i.e. under optimal condition for 3'-processing activity when using the viral sequence: [DNA] = 5 nM and [IN] = 200 nM (in the same buffer used for DNA-binding assay).

Determination of zinc release by DIBA-1

The ejection of zinc from IN was quantified using the chromophoric chelator 4-(2-pyridylazo)resorcinol (PAR) (Sigma). Zn²⁺ release by DIBA-1 was monitored by absorbance using a Uvikon 941 (Kontron) spectrophotometer as the formation of the Zn²⁺-(PAR)₂ complex enhances absorbance at 495 nm. All experiments were conducted in a Tris buffer (20 mM, pH 7.0) containing 15% DMSO (v/v) to improve the solubility of DIBA-1. The molar extinction coefficient of the Zn²⁺-(PAR)₂ complex was measured in the presence of DMSO (15%) using zinc solutions of known concentrations (from 1 to 6 μM). A molar extinction coefficient of 6.1 10⁴ M⁻¹ cm⁻¹ was found in 15% DMSO, a value slightly lower than the one previously found in water (6.6 10⁴ M⁻¹ cm⁻¹) (37).

Characterization of DIBA-1 modified IN by mass spectrometry

The covalent modification of IN by DIBA-1 was evaluated using in-gel tryptic digestion and SELDI mass spectrometry analysis. To enhance the enzymatic digestion, we used the ProteaseMAXTM Surfactant, Trypsin Enhancer (Promega, France) as described by the manufacturer. IN (20 μM), preincubated or not with DIBA-1 (40 μM) in 20 mM HEPES (pH 6.9), DMSO 15% (v/v), NaCl 400 mM, was subjected to SDS-PAGE electrophoresis (without DTT). After Coomassie staining, the gel slides were destained twice in 50 mM

NH_4CO_3 , 50% methanol (v/v) (200 μl) for 1 min, in 50 mM NH_4CO_3 , 50% acetonitrile (v/v) (200 μl) for 5 min and, finally, dried in a Speed Vac. No DIBA-1-mediated inter-molecular crosslink was evidenced by gel-electrophoresis. The gel slides were then rehydrated in a NH_4CO_3 (50 mM) solution containing 12 ng/ μl trypsin and 0.025% ProteaseMAXTM Surfactant, for 10 min, and further incubated overnight (protocol A: PA) or 2 h (protocol B: PB) at 37°C. The resulting peptides were recovered either by addition of a 10 μl solution containing 0.01% ProteaseMAXTM Surfactant in NANOpure[®] water (PA) or by concentration/purification using Zip Tip C18 (Millipore) [Elution with a 80% acetonitrile (v/v), 0.1% TFA solution] (PB), and spotted onto a SEND-ID protein array according to CIPHERGEN's protocol. The mass spectra were obtained by reading the protein chip using a SELDI mass spectrometer. The resulting spectra were compared with the *in silico* profile obtained with GPMaw software (Lighthouse Data).

RESULTS

We have previously shown that IN binding to an oligonucleotide mimicking the HIV-1 U5 DNA extremity was cooperative in the presence of Mg^{2+} and characterized by a Hill coefficient of 2 (18), consistent with both time-resolved fluorescence anisotropy (3,5) and cross-linking (2) experiments showing that a dimer of IN corresponds to the catalytically active form for the 3'-processing reaction. This result supports a model in which the dimer originates from the cooperative assembly of two protomeric units on the viral DNA end (3,5,38). In the present study, we addressed the question of whether the above-mentioned cooperative property was dependent or not on the DNA sequence context (viral versus random) or the nature of the metallic cofactor (Mg^{2+} versus Mn^{2+}).

The cooperative binding of IN to DNA is modulated by the cofactor and the DNA sequence

We used steady-state fluorescence anisotropy for monitoring IN–DNA interaction as previously described (3,18,36). IN binding to the viral DNA sequence (U5A/U5B) was characterized by a Hill coefficient (\tilde{n}) of 1.97 in the presence of Mg^{2+} (Table 1), indicating cooperativity, in accordance with our previous study (18). It was previously shown that the 3'-processing activity is much more sensitive to the viral DNA sequence in the Mg^{2+} context than the Mn^{2+} context, suggesting that specific contacts between IN and the viral DNA extremity are more favored in the presence of Mg^{2+} (12,13). To gain insight into the cooperativity–specificity relationship, we first tested whether the cooperative property was dependent or not on the nature of the metallic cofactor. Using the cognate viral DNA sequence (U5A/U5B), we found that Mg^{2+} - and Mn^{2+} -dependent DNA-binding display different Hill coefficients, with a DNA-binding process that is more cooperative in the presence of Mg^{2+} ($\tilde{n} = 1.97$ and 1.29 for Mg^{2+} and Mn^{2+} , respectively; Table 1). It is important to note that IN does not strictly require a

divalent cation for DNA binding (3,25). It was then possible to assess the cooperative behaviour of IN in the absence of metallic cofactor. The corresponding \tilde{n} value ($\tilde{n} = 1.34$) (see also Table 4) was found to be similar to the value obtained with Mn^{2+} ($\tilde{n} = 1.29$). The concentration of Mg^{2+} compatible with cooperativity was found in the 5–15 mM concentration range (the IN–DNA interaction is significantly reduced above 15 mM Mg^{2+}).

We next assessed whether IN binding to non-specific random DNA sequences was cooperative or not. Two random sequences were tested (RAND1A/RAND1B or RAND2A/RAND2B). In the presence of Mg^{2+} , the Hill coefficient was significantly reduced when using these DNA sequences ($\tilde{n} \approx 1.2$; Table 1). Clearly, the cooperative DNA-binding mode ($\tilde{n} = 1.97$) requires both the cognate viral sequence and Mg^{2+} as a cofactor: Mn^{2+} -dependent DNA binding on the cognate sequence or Mg^{2+} -dependent DNA binding on the random DNA sequences significantly decreased the Hill number. Moreover, cooperativity was totally abolished with Mn^{2+} and a random DNA sequence ($\tilde{n} \approx 0.9$ –0.92; Table 1). Similar results were obtained with the wild-type protein and the C280S mutant (used throughout the rest of this article; see below). Importantly, the modulation of the Hill number was not correlated to a change in the degree of IN oligomerization. In fact, the long rotational correlation times (θ) [as monitored by time-resolved fluorescence anisotropy (3)], characterizing the following complexes: IN- Mg^{2+} -viral sequence, IN- Mn^{2+} -viral sequence, IN- Mg^{2+} -random sequence, were not significantly different (Table 2): All θ values (in the 39–44 ns range at 25°C) were compatible with a dimeric form of IN bound to DNA, in agreement with our previous study of the IN- Mg^{2+} -viral DNA complex [$\theta = 37.8$ ns in (3)].

Taken together, our results show that the formation of specific IN–DNA complexes is concomitant to the presence of a cooperative DNA-binding mode. Of particular interest is the observation that cooperativity measurements allow to distinguish between specific and non-specific DNA-binding modes. Nevertheless, we observed only a slight difference in the apparent $K_{d,\text{app}}$ values between Mg^{2+} and Mn^{2+} ($K_{d,\text{app}} = 65$ and 51 nM, respectively; Table 3, first line) and we did not observe any significant difference in the $K_{d,\text{app}}$ values between the different sequences for a given metallic cofactor (data not shown). Moreover, the $K_{d,\text{app}}$ value in the absence of divalent cation was found to be 40 nM (Table 3), confirming that the presence of either metallic cofactor is not crucial for the overall DNA-binding process. Therefore, the nature of the metallic cofactor or the DNA sequence has no significant influence on the overall IN–DNA affinity, suggesting that non-specific contacts constitute the main driving force for the complex stability, while specific contacts, probably mediated by a cooperative mechanism of assembly, are essential for fine positioning of IN with respect to the cleavage site and subsequent catalysis. It has been reported that $\text{Mg}^{2+}/\text{Mn}^{2+}$ stimulate the preferential recognition of the cognate sequence by HIV-1 IN (as shown by the decrease in the K_d -value measured by SPR assay)

(24). One possible reason to explain this apparent contradiction with our data is that the study by Yi and collaborators was carried out at high ionic strength (300 mM), while our experiments were conducted under low ionic strength conditions (50 mM). Indeed, we have previously shown that ionic strength selectively disrupts non-specific IN–IN interactions, using PFV-1 IN, accounting for the observed differential DNA binding between viral and random sequences at 150 mM NaCl, while no difference was evidenced at 50 mM NaCl (5). Such a differential DNA binding was not observed for HIV-1 IN, even at 150 mM NaCl (5). This is explained by the lower propensity of PFV-1 IN to mediate non-specific IN–IN interactions, and probably, a higher ionic strength (i.e. 300 mM) is required in the case of HIV-1 IN to distinguish between specific and non-specific complexes in terms of affinity. However, it is important to note that fluorescence anisotropy experiments did not show any binding of

HIV-1 IN to DNA at 300 mM NaCl (up to 3 μ M IN) (data not shown). Further investigation is required to understand the exact reason of this discrepancy between SPR and fluorescence anisotropy results.

Zinc ejection by DIBA-1 influences the cooperative binding of IN to the DNA substrate but does not prevent IN–DNA interactions

Taking into account that zinc promotes the Mg^{2+} -dependent activity of IN and has no or a modest influence on the Mn^{2+} -dependent activity (28,29), we next assessed whether zinc ejection may influence the cooperative DNA-binding properties of IN, using DIBA-1 (Figure 1A), a zinc ejector compound that can react with zinc fingers (33). In the following sections, we tested the effect of DIBA-1 in the context of the C280S mutation, taking into consideration that (i) purification and assay buffers were non-reducing (without DTT and β -mercaptoethanol) to avoid DIBA-1 reduction, (ii) the C280 residue was described to be responsible for the formation of covalent multimers under non-reducing conditions (35), (iii) the C280S mutation does not affect viral replication or *in vitro* IN activity (35). We first tested whether DIBA-1 ejected zinc from IN by spectroscopy using the chromophoric chelator 4-(2-pyridylazo)resorcinol (PAR). Figure 1B clearly shows that DIBA-1 triggered zinc release from IN (confirmed below by mass spectroscopy analysis demonstrating that DIBA-1 targets the HHCC motif). This effect was counteracted by a reducing agent such as β -mercaptoethanol (Figure 1B). According to the molar extinction coefficient of Zn^{2+} –(PAR)₂

Table 2. Long correlation times characterizing different IN–DNA complexes^a

DNA sequence	U5A/U5B	U5A/U5B	RAND1A/ RAND1B
Metallic cofactor ^b	Mg^{2+}	Mn^{2+}	Mg^{2+}
Long correlation time	39.1 ± 4.5 ns	43.9 ± 5.1 ns	41.4 ± 4.8 ns

^aObtained at 25°C with [IN] = 200 nM and [DNA] = 5 nM (see ‘Materials and Methods’ section).
^b10 mM.

Table 3. $K_{d,app}$ values for DNA-binding of the full-length and truncated IN in the presence or absence of DIBA-1^a

IN	$K_{d,app}$, nM					
	10 mM Mg^{2+}		10 mM Mn^{2+}		No divalent cation	
	DIBA–	DIBA + ^b	DIBA–	DIBA + ^b	DIBA–	DIBA + ^b
Full-length	65 ± 7	65 ± 9	51 ± 7	53 ± 5	40 ± 15	48 ± 11
ΔN	45 ± 7	45 ± 6	28 ± 3	29 ± 6	ND	ND
ΔC	531 ± 188	652 ± 214	60 ± 4	64 ± 8	ND	ND
CC	233 ± 98	279 ± 34	53 ± 13	61 ± 10	ND	ND

^aThe DNA sequence corresponds to the HIV-1 U5 extremity (U5A/U5B) (see ‘Materials and Methods’ section).

^bCorresponding to a DIBA-1:IN ratio of 3:1.

ND, not determined.

Table 4. Hill coefficients for DNA-binding of the full-length and truncated IN in the presence or absence of DIBA-1^a

IN	Hill coefficient					
	10 mM Mg^{2+}		10 mM Mn^{2+}		No divalent cation	
	DIBA–	DIBA + ^b	DIBA–	DIBA + ^b	DIBA–	DIBA + ^b
Full-length	1.97 ± 0.10	1.47 ± 0.02	1.29 ± 0.09	1.20 ± 0.10	1.34 ± 0.08	1.37 ± 0.09
ΔN	1.45 ± 0.12	1.41 ± 0.10	1.20 ± 0.06	1.30 ± 0.13	ND	ND
ΔC	1.90 ± 0.10	1.43 ± 0.12	1.24 ± 0.07	1.21 ± 0.11	ND	ND
CC	1.38 ± 0.09	1.32 ± 0.06	1.26 ± 0.13	1.20 ± 0.05	ND	ND

^aThe DNA sequence corresponds to the HIV-1 U5 extremity (U5A/U5B) (see ‘Materials and Methods’ section).

^bCorresponding to a DIBA-1:IN ratio of 3:1.

complex in 15 % DMSO ($6.1 \times 10^4 \text{ M}^{-1} \text{ cm}^{-1}$) and the IN concentration (1 μM), the absorbance value at the plateau (0.055) indicates a zinc content of 0.9 eq Zn^{2+} per IN monomer, in agreement with the expected value for a protein encompassing one zinc-finger domain. Moreover, we found that the reaction of two DIBA-1 molecules per IN monomer coincides with zinc release (Figure 1C). This result will be further discussed (see 'Discussion' section).

The DIBA-1-mediated zinc ejection from IN prompted us to study the influence of DIBA-1 on the catalytic activity of IN. DIBA-1 strongly inhibited the 3'-processing and disintegration catalyzed by the full-length IN with IC_{50} values of 11–15 nM for both reactions in the presence of Mg^{2+} (Figure 2A–D). The IC_{50} values were significantly higher in the presence of Mn^{2+} (115–126 nM). All these reactions were carried out in the absence of reducing agent to prevent DIBA-1 reduction. Indeed, adding DTT or β -mercaptoethanol to the reaction mixture blocked the DIBA-1 inhibitory effect (Figure 2E). Recently, it has been reported that complexation reactions between bis(2-bromophenyl)disulfide and transition metal ions, including manganese, may occur (39). To address the question of the possible complexation between DIBA-1 and Mn^{2+} —which could explain the higher IC_{50} values obtained in the presence of Mn^{2+} compared to Mg^{2+} —we tested the influence of the order of addition of the reagents on the IC_{50} value. Three different preincubation protocols were tested (see 'Materials and Methods' section). No significant influence of the order of addition of the reagents on the IC_{50} values was observed, i.e. the three protocols lead to similar IC_{50} values for a given metallic cofactor. In particular, for Mn^{2+} , the comparison between protocols 1 (when DIBA-1 is preincubated with Mn^{2+} before addition of IN and DNA) and 2 (when DIBA-1 is preincubated with IN before addition of Mn^{2+} and DNA) suggests that, under our experimental conditions, Mn^{2+} does not interact or only weakly interacts with DIBA-1, to an extent that does not significantly affect the concentration of free DIBA-1 molecules, available to react with IN. Moreover, the similar IC_{50} values obtained between protocols 2 and 3 (when IN is preincubated with the metallic cofactor before addition of DIBA-1 and DNA), indicates that the binding of either Mn^{2+} or Mg^{2+} to IN is not a prerequisite for the reaction of DIBA-1 with IN. Altogether, these data suggest that the influence of the cofactor context on the IN inhibition by DIBA-1, is not explained by a substantial decrease in the effective concentration of the inhibitor in the presence of Mn^{2+} .

We next performed DNA-binding assays to test whether DIBA-1 could inhibit IN activity via inhibiting the IN–DNA interaction (i.e. DIBA-1 behaves as a competitive inhibitor), as found for the compounds of the styrylquinoline family (INBI) (18), or acts at the catalytic step (post-DNA-binding step event). Increasing concentrations of the full-length IN were added to a fluorescein-labeled DNA that mimics the HIV-1 U5 DNA extremity and fluorescence anisotropy was measured in the absence (Figure 3, top, black squares) or presence (white squares) of DIBA-1 at a constant DIBA-1:IN ratio (2:1). Results clearly show that

DIBA-1 did not prevent the DNA binding of IN. The corresponding 3'-processing activities are also reported for each condition and confirm that DIBA-1 did efficiently inhibit 3'-processing activity under conditions that did not significantly affect the amount of IN–DNA complexes (Figure 3, top, compare black and white circles). The apparent K_d -values for the full-length protein were similar, regardless of the metallic cofactor used, and independent of the presence of DIBA-1 (Table 3, first line), confirming that DIBA-1 allows IN to bind to its DNA substrate but inactivates the formed complexes. This result is in sharp contrast to the one previously observed with styrylquinoline compounds (such as FZ55, Khd161 and FZ41) for which the inhibition of the 3'-processing activity was found to closely parallel the inhibition of the formation of IN–DNA complexes as monitored by fluorescence anisotropy (3,18). We then tested and compared FZ41 and DIBA-1 for their inhibitory effects on the DNA binding step (as monitored by fluorescence anisotropy), under the same experimental conditions, i.e. by using a Tris:DMSO mixture (85:15) (v/v) containing constant concentrations of IN and DNA, and increasing concentrations of drugs (Figure 3, bottom). FZ41 was found to inhibit the binding of IN to DNA with an IC_{50} value of 0.75 μM (black triangles), in agreement with the IC_{50} value characterizing the 3'-processing inhibition (3,40). This result confirms that the inhibition of the 3'-processing activity by styrylquinoline compounds is fully explained by the prevention of IN–DNA recognition. In contrast, no inhibition of the IN–DNA interaction was evidenced with DIBA-1 using the same DNA-binding assay (white squares).

Remarkably, even though DIBA-1 had no measurable effect on the overall affinity, it significantly reduced the Hill coefficient from 2 to 1.47 (Figure 4 and Table 4), suggesting that DIBA-1 interferes with the cooperative binding of IN to DNA. As mentioned above, such a cooperative binding was not observed in the presence of Mn^{2+} or in the absence of divalent cation ($\tilde{n} = 1.29$ and 1.34, respectively), and DIBA-1 did not further change these \tilde{n} values ($\tilde{n} = 1.20$ and 1.37, respectively) (Table 4). This result suggests that the DIBA-1 effect on the cooperative DNA-binding mode is strongly related to the differential inhibition by DIBA-1 of Mn^{2+} - and Mg^{2+} -dependent IN activities, as above-mentioned [a better inhibitory effect, ≈ 10 -fold, was systematically found in the Mg^{2+} context compared to Mn^{2+} (Figure 2)]. Altogether, our results show that the N-terminal domain and its HHCC motif do not play a direct role in terms of affinity/stability of the IN–DNA complex, but, most likely, account for the observed Mg^{2+} -dependent cooperative behavior of IN via protein–protein interactions. We also compared the DNA-binding properties of the full-length IN with truncated proteins: IN^{50–288} (ΔN), IN^{1–213} (ΔC) and IN^{50–213} (CC). All proteins were able to bind to the DNA substrate (Table 3), although truncated proteins are inactive for 3'-processing. The C-terminal domain plays a key role for the affinity of the IN–DNA complex but only in the Mg^{2+} context, whereas the $K_{d,\text{app}}$ values in Mn^{2+} were all similar (Table 3, lines 3 and 4). This finding agrees with previous works showing that the C-terminal

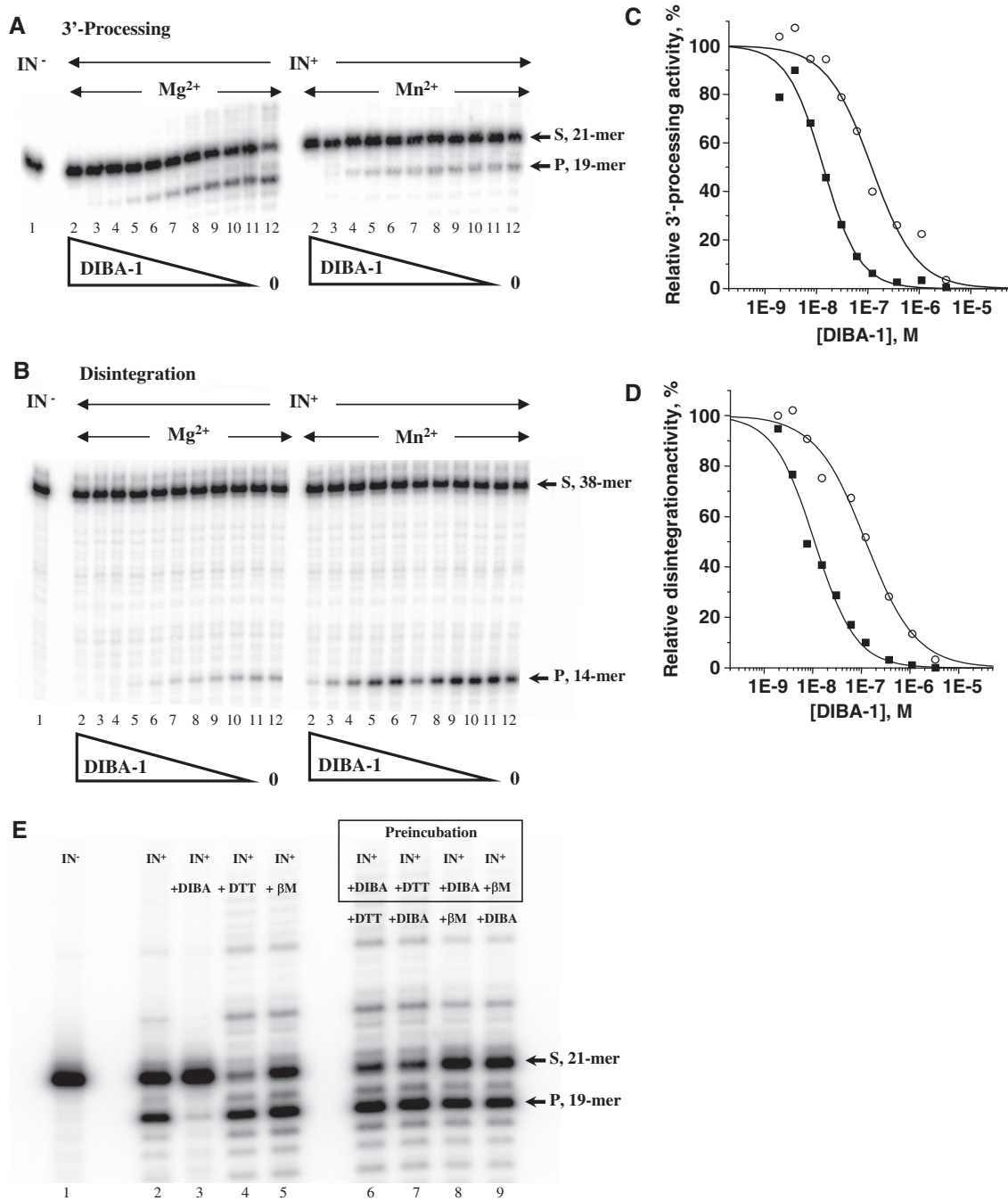


Figure 2. Inhibition of 3'-processing and disintegration by DIBA-1. 3'-Processing (A) or disintegration (B) reactions were performed in the presence of DIBA-1 with either 10 mM Mg²⁺ (left) or 10 mM Mn²⁺ (right), full-length IN (50 nM) and DNA substrate (1 nM) (except lane 1: no integrase). DIBA-1 concentration was 0 (lane 12), 1.9 nM (lane 11), 3.8 nM (lane 10), 7.7 nM (lane 9), 15.4 nM (lane 8), 30.8 nM (lane 7), 61.5 nM (lane 6), 123 nM (lane 5), 370 nM (lane 4), 1111 nM (lane 3) or 3333 nM (lane 2). S, DNA substrate. P, DNA product. Relative activities of 3'-processing (C) or disintegration (D) (with either Mg²⁺, black squares; or Mn²⁺, white circles, as a metallic cofactor) were plotted against the DIBA-1 concentration. In the presence of Mg²⁺, the calculated IC₅₀ values were 13 and 11 nM for 3'-processing and disintegration reactions, respectively. The corresponding values in the presence of Mn²⁺ were 118 and 123 nM, respectively. Similar results were obtained regardless of the preincubation protocol used (1, 2 or 3; see 'Materials and Methods' section). (E) Effect of reducing agents on the inhibitory activity of DIBA-1. 3'-Processing reaction was performed using full-length IN (100 nM), DNA substrate (1 nM) and Mg²⁺ (10 mM) as a cofactor (lanes 2–9). IN was preincubated (for 10 min at room temperature) alone (lane 2), with DIBA-1 (lane 3) or DTT (lane 4) or β-mercaptoethanol (lane 5), before addition of Mg²⁺ and DNA; lanes 6 and 8, IN/Mg²⁺ was preincubated with DIBA-1 for 10 min at room temperature before adding the reducing agent and DNA (lane 6, DTT; lane 8, β-mercaptoethanol); lanes 7 and 9, IN/Mg²⁺ was preincubated with the reducing agent (lane 7, DTT; lane 9, β-mercaptoethanol) for 10 min at room temperature before adding DIBA-1 and DNA. Concentrations of DTT and β-mercaptoethanol were 4 mM. Concentration of DIBA-1 was 200 nM. Lane 1, DNA alone.

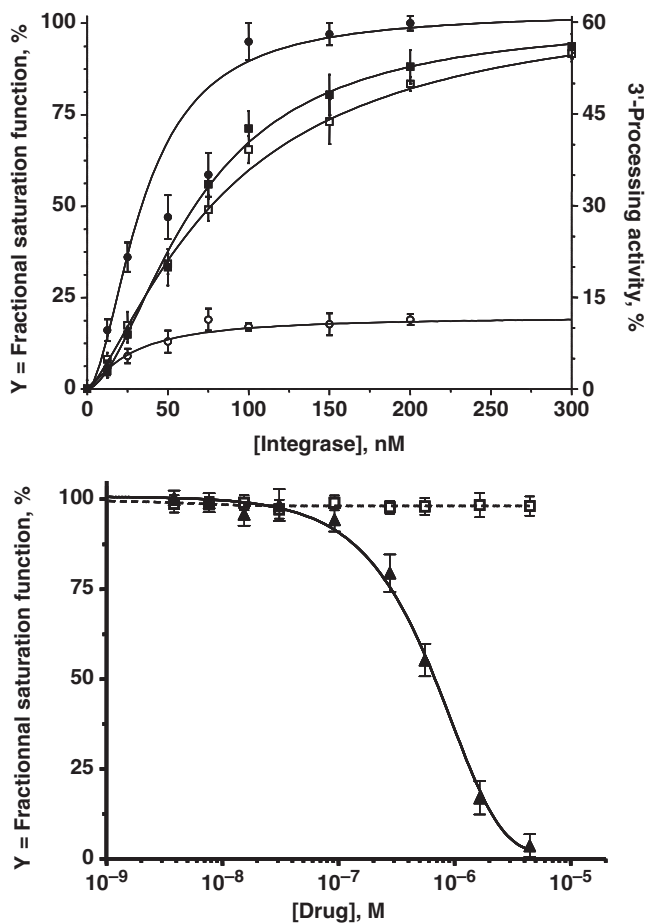


Figure 3. DIBA-1 does not prevent formation of IN–DNA complexes. Top, increasing concentrations of IN were incubated with DNA substrate (1 nM) in a Tris buffer (20 mM, pH 7.0) containing 15% DMSO (v/v), NaCl 50 mM and 10 mM Mg^{2+} . Left axis, the DNA binding step was recorded by fluorescence anisotropy as described in ‘Materials and Methods’ section. Black squares, no DIBA-1. White squares, [DIBA-1]:[IN] = 2: 1. Right axis, 3'-processing activity for IN/DNA mixtures (measured as described in ‘Materials and Methods’ section with preincubation conditions corresponding to protocol 3). Black circles, no DIBA-1. White circles, [DIBA-1]:[IN] = 2: 1. Similar qualitative profiles were obtained using Mn^{2+} as a cofactor, but with a less potent inhibition of the 3'-processing reaction, according to Figure 2 (data not shown). Bottom: IN (120 nM) was incubated with DNA substrate (1 nM) in a Tris buffer (20 mM, pH 7.0) containing 15% DMSO (v/v), NaCl 50 mM, 10 mM Mg^{2+} , and increasing concentrations of either FZ41 (black triangles) or DIBA-1 (white squares). The binding of IN to DNA was monitored by fluorescence anisotropy.

domain is critical for overall IN–DNA complex stability. However, the differential influence of the divalent cations on the affinity also suggests that this domain could be involved in specific interactions with DNA, assuming that Mg^{2+} -dependent catalysis is more sequence-specific than Mn^{2+} -dependent catalysis (12,13). In contrast, the role of the N-terminal domain in the complex stability appears to be much less important as its deletion does not decrease the affinity, consistent with the absence of any significant effect of zinc ejection on the $K_{d,app}$ values. There is rather a slight increase in the affinity (decrease in the $K_{d,app}$ value) upon deletion of the N-terminal domain (Table 3; compare the full-length to

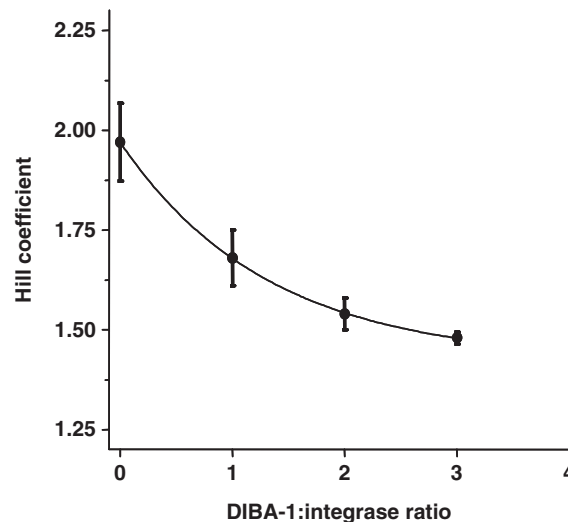


Figure 4. Hill coefficient as a function of the DIBA-1:IN ratio. DNA-binding isotherms were recorded as described in the legend of Figure 3.

the ΔN protein—lines 1 and 2—and compare the ΔC to the CC protein—lines 3 and 4).

Regarding the Hill coefficients characterizing truncated proteins in the presence of Mg^{2+} (Table 4), only ΔC displayed high cooperativity ($\tilde{n} = 1.9$) as the full-length IN. In contrast, ΔN and CC proteins, lacking the N-terminal domain, were characterized by lower \tilde{n} values (1.45 and 1.38, respectively). Importantly, the Hill coefficient of the ΔC protein significantly decreased in the presence of DIBA-1 ($\tilde{n} = 1.43$), in a similar manner to that of the full-length IN, whereas DIBA-1 did not further decrease the \tilde{n} values of the ΔN and CC proteins (1.41 and 1.32, respectively). Moreover, as found with the full-length IN, the Hill coefficients of all truncated proteins were lower in the presence of Mn^{2+} (1.20–1.26) and were not influenced by the presence of DIBA-1.

In conclusion, DIBA-1 did not prevent the formation of IN–DNA complexes, but, in the Mg^{2+} context, significantly changed the Hill coefficient, suggesting that the nature of the IN–IN interaction onto the DNA substrate or the oligomeric status of the IN–DNA complex is modulated by DIBA-1. Altogether, our results show that the N-terminal domain mainly mediates the cooperative binding of Mg^{2+} -bound IN to the cognate DNA sequence. However, the Mn^{2+} -dependent 3'-processing and disintegration activities performed by full-length IN remained sensitive to DIBA-1, albeit less sensitive than Mg^{2+} -dependent activities, suggesting that the loss of cooperativity does not fully explain the IN inhibition, especially in the Mn^{2+} context. To better understand the IN domains involved in the DIBA-1 response, we next tested the DIBA-1 effect on truncated INs such as double-domain proteins, ΔN and ΔC , as well as the single-domain catalytic core, CC. We used the disintegration assay to test activity in the presence of Mn^{2+} , which is required for disintegration activity of truncated proteins, as these proteins cannot catalyze the 3'-processing or Mg^{2+} -dependent disintegration (11). All

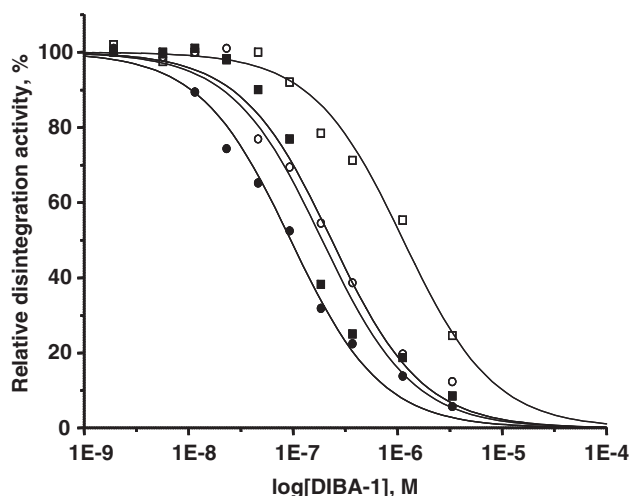


Figure 5. Effect of DIBA-1 on the full-length IN and truncated mutants. Disintegration reactions were performed in the presence of 10 mM Mn^{2+} as described in 'Materials and Methods' section (the preincubation step was carried out according to protocol 3). Relative activities of disintegration were plotted against the DIBA-1 concentration (black circles, full-length IN; white circles, ΔN ; white squares, ΔC ; black squares, CC). The calculated IC_{50} values were 95, 234, 1135 and 191 nM for full-length, ΔN , ΔC and CC proteins, respectively. Protein and DNA substrate concentrations were 50 nM and 1 nM, respectively.

truncated proteins, including CC, remained inhibited by DIBA-1, but with higher IC_{50} values than the full-length IN (Figure 5). Therefore, the inhibition does not strictly require the zinc-finger, as DIBA-1 can still inhibit truncated mutants lacking the N-terminal domain. This result highlights another effect of DIBA-1, i.e. DIBA-1 can directly affect the catalytic core, independent of zinc ejection.

Mass spectrometry analysis of IN–DIBA-1 complexes: the DIBA-1 compound covalently targets both the N-terminal HHCC motif and the catalytic core

SELDI-MS analysis of the full-length IN was performed after a trypsin digestion of IN with or without DIBA-1. A protein coverage of $\sim 92\%$ was obtained, regardless of the protocol used (PA or PB; see 'Materials and Methods' section) (Figure 6A). The molecular mass of two peptides was modulated by DIBA-1 (using PA or PB) (Figure 6B). The first one (pos. 35/42) contained the Cys 40 residue, confirming that DIBA-1 targets at least one cysteine residue in the N-terminal HHCC motif. The second peptide (pos. 47/71) contained both Cys 56 and Cys 65, confirming that the catalytic core is also targeted by DIBA-1. Additionally, our results show that the Cys 130 residue is not targeted by DIBA-1 as no influence of DIBA-1 was evidenced on peptides 112/136 and 128/136 (with PA or PB) (Figure 6C). Using PA, no adduct species were evidenced, probably for hydrophobicity reasons, even though the peptides 35/42 (MW, 864 Da) and 47/71 [MW, 2711 Da; MW(+16), 2727 Da] were reproducibly absent in samples treated with DIBA-1. In contrast, an adduct product was observed using PB (MW, 3034 Da), corresponding to a

covalent complex between the oxidized peptide 47/71 (MW(+16), 2727 Da) and a DIBA-1 monomer (MW, 307 Da) (no adduct product related to the 35/42 peptide was detected, even using PB). This product corresponds however to a minor species (data not shown). Importantly, a dominant adduct product (MW, 3795 Da; MW(+16), 3811 Da) was concomitantly observed only with samples treated with DIBA-1 (using PB) (Figure 6D): This product originates from a miscleavage leading to a peptide [pos. 43/71; MW, 3182 Da; MW(+16), 3198 Da] covalently modified by DIBA-1. The MW difference (+614 Da) suggests that two of the three cysteine residues contained in this peptide (C43, C56, C65) are involved in a covalent complex with a DIBA-1 monomer (+307 Da per cysteine) according to the general mechanism proposed by Loo *et al.* (41) (see also Figure 6E). This result also suggests that the tryptic proteolysis occurring at K46 is altered in DIBA-1-treated samples (no unmodified 43/71 peptide was found in untreated samples). Altogether, our results indicate that DIBA-1 covalently targets three cysteine residues within IN, (i) Cys 40 and Cys 43 in the HHCC motif and, (ii) Cys 56 or Cys 65 in the central domain. The results were similar regardless of the divalent cation used (Mg^{2+} or Mn^{2+}). Thus, DIBA-1 targets both the zinc-finger motif in the N-terminal domain and the active site in the CC domain and the nature of the metallic cofactor does not influence the binding profile of DIBA-1.

To discriminate between Cys 56 and Cys 65, we performed site-directed mutagenesis. The C56S, C65S and C56S-C65S mutants were generated (in the context of the C280S mutation) and tested for DIBA-1 sensitivity. The three mutants display similar 3'-processing activity as the native protein (C280S only) (data not shown). DIBA-1 inhibited the C65S mutant in Mn^{2+} with a similar IC_{50} as the native protein (Table 5). In contrast, DIBA-1 inhibition was much less potent with C56S and C56S/C65S mutants, indicating the importance of the Cys 56 residue in DIBA-1 binding and, then, in mediating the inhibition of IN activity. Accordingly, it was shown by others that modifying Cys 56 by N-ethylmaleimide similarly inactivates IN (42). This finding was confirmed by the MS analysis of the C56S mutant. In contrast to the result obtained with the C56 protein, no influence of DIBA-1 on the molecular mass of the 47/71 peptide was evidenced with the S56 protein (only the molecular mass of the 35/42 peptide was modulated by DIBA-1) (data not shown). Moreover, no adduct species equivalent to either the 3034 Da (MW_{eq} , 3019 Da for S56) or the 3795(+16) Da product [MW_{eq} , 3780(+16) Da for S56], previously identified with the C56 protein (using PB), were evidenced with S56 under similar experimental conditions. Similar MS results were obtained, regardless of the cofactor used. However, regarding the inhibition of 3'-processing, results were different in Mg^{2+} compared to Mn^{2+} : DIBA-1 was equally potent in all mutants (only a modest increase of the IC_{50} value was observed with the C56S or the C56S-C65S mutant), and more potent than in Mn^{2+} (Table 5). This suggests that the consequence of DIBA-1 binding to the N-terminal domain (i.e. zinc ejection) dominates in Mg^{2+} and that this mechanism

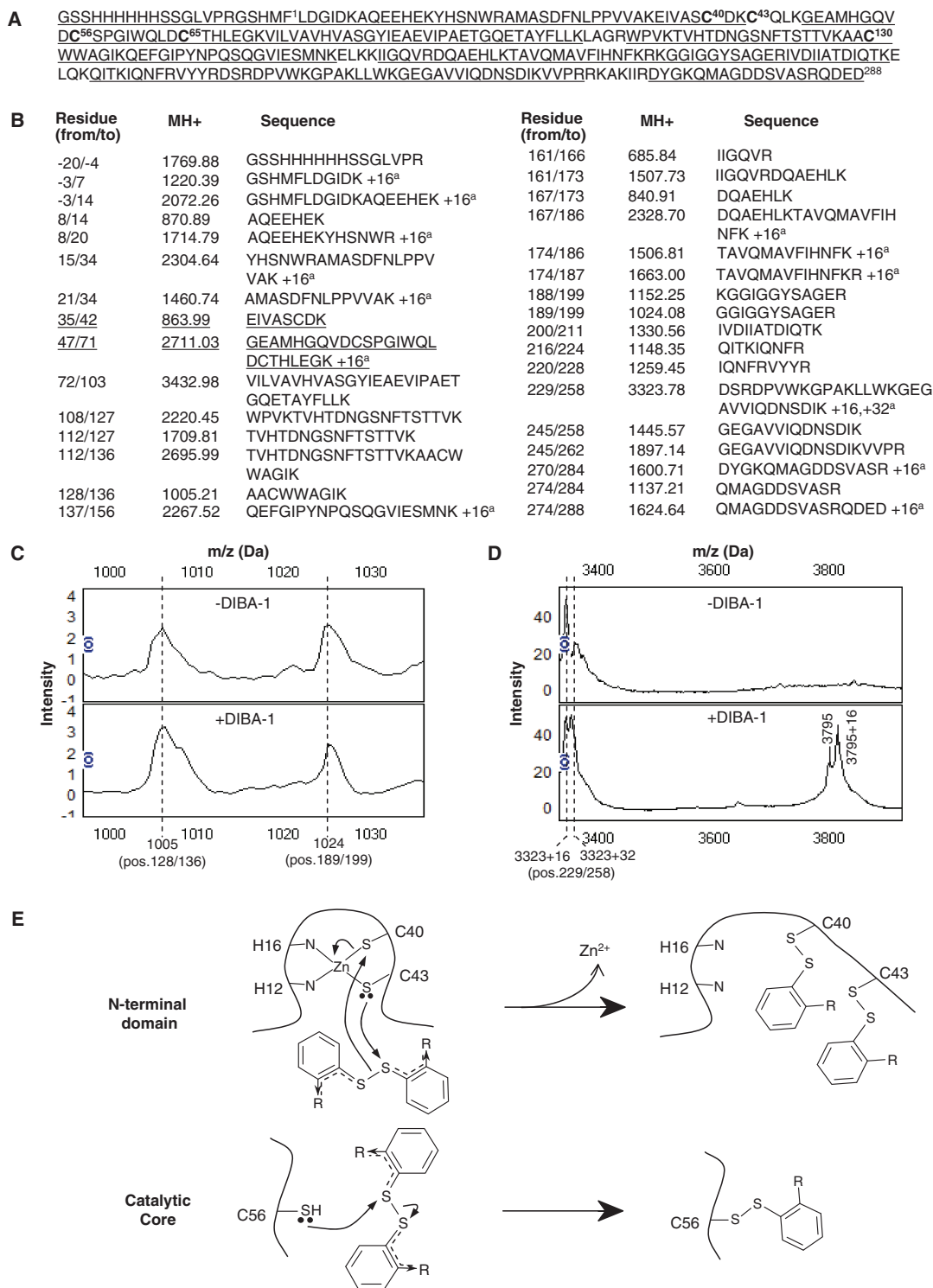


Figure 6. SELDI analysis of in-gel proteolysis of DIBA-1 modified IN. The SELDI analysis of trypsin digestion of HIV-1 IN, treated or not with DIBA-1, was carried out as described in 'Materials and Methods' section. (A) Primary sequence of HIV-1 IN. The tryptic peptides obtained after proteolysis were analyzed using a SEND-ID protein chip. The protein coverage was 92% (corresponding sequences are underlined). (B) Sequences of the recovered peptides for IN sample not treated with DIBA-1. The underlined sequences correspond to shifted m/z peaks when IN was initially treated with DIBA-1 before in-gel proteolysis. 'a +16' or '+16, +32' means that the same peptide can be represented by two or three peaks, respectively: The first one corresponds to the non-oxidized form. The second and the third peak correspond to the presence of one or two oxidized residues (methionine or tryptophan) resulting in a mass shift of +16 or +32 Da, respectively. (C and D) MS spectra magnified in two regions of interest (top, untreated sample; bottom, DIBA-1-treated sample), showing that: (C) DIBA-1 had no effect on the 128/136 peptide (MW, 1005 Da) containing the C130 residue [a similar result was obtained with the 112/136 peptide (MW, 2696 Da) (data not shown)]; (D) A new peak [MW, 3795 (+16) Da] was identified in the presence of DIBA-1, compatible with the formation of a covalent complex between the 43/71 peptide [MW, 3182.63 (+16) Da] and two DIBA-1 monomers (MW, 2×307 Da) (see text for details). (E) Models for the reaction pathways involving DIBA-1 and: (i) the IN HHCC motif in the N-terminal domain (top), (ii) the Cys 56 residue of the catalytic core domain (bottom).

Table 5. IC₅₀ values characterizing IN inhibition (3'-processing reaction) by DIBA-1 obtained with different cysteine mutants^a

Metallic cofactor ^b	IC ₅₀ , nM			
	C280S	C65S, C280S	C56S, C280S	C56S, C65S, C280S
Mg ²⁺	14 ± 3	12 ± 2	19 ± 4	24 ± 5
Mn ²⁺	126 ± 16	116 ± 13	1155 ± 547	566 ± 186

^aIN activity was measured as described in 'Materials and Methods' section with preincubation conditions corresponding to protocol 3.

^b10 mM.

fully accounts for the inhibition of the Mg²⁺-dependent activity of IN. In contrast, zinc ejection and its consequence on the cooperative DNA-binding properties of IN are neutral in terms of catalysis in the Mn²⁺ context according to (30), and thus, catalytic performance becomes more sensitive to perturbation of the active site in Mn²⁺. The Mn²⁺-dependent activity is then primarily affected by the direct reaction of DIBA-1 with the catalytic core via the Cys 56 residue. Finally, as found for the native protein, DIBA-1 did not affect the DNA-binding step of the C56S, C65S and C56S-C65S mutants, regardless of the cofactor context (data not shown).

DISCUSSION

We have characterized the cooperative DNA-binding property of HIV-1 IN to understand the structural determinants of the reaction specificity at the DNA binding level. To date, only the central catalytic domain was clearly shown to be directly involved in the specific recognition of the viral DNA substrate (12,43,44), although no significant difference in terms of affinity between cognate and non-specific random sequences can be evidenced in most current DNA binding assays. Consistently, mutations of some residues, known to be involved in such specific contacts and essential for activity—for instance, the Q148 or Y143 residue—do not dramatically alter the formation of IN–DNA complexes (12,22,23). In this study, we show that the IN N-terminal domain, containing a pseudo zinc finger, plays also a key role, at least indirectly, for the formation of specific IN–DNA contacts. The HHCC motif mediates a cooperative DNA binding that occurs only in the presence of the cognate viral sequence and the physiologically relevant Mg²⁺ cofactor. Furthermore, we found that DIBA-1, a zinc ejector compound, induced a significant decrease in cooperativity, dependent on the ejection of zinc from the N-terminal HHCC motif and, concomitantly, severely impaired the 3'-processing activity. However, our results indicate a second mode of action of DIBA-1 for inhibiting catalytic activity that is independent of zinc ejection but requires a direct interaction with the central domain. This second mechanism explains why DIBA-1 retained the ability to inhibit the Mn²⁺-dependent activity—even though less efficiently compared to Mg²⁺-dependent

activity—since the Mn²⁺-dependent DNA binding was principally non-cooperative. Although DIBA-1 covalently targets both the N-terminal and the central domains, regardless of the metallic cofactor (Mg²⁺ or Mn²⁺), the relative contribution of each mechanism to the inhibition of catalytic activity depends on the metallic cofactor initially bound to IN. Taken together, our data indicate that the cooperative assembly of IN/DNA complexes is important for the Mg²⁺-dependent activity, but dispensable in the Mn²⁺ context. The DIBA-1-dependent zinc ejection from the HHCC motif is responsible for the reduction of cooperativity and the potent inhibitory effect of DIBA-1 in Mg²⁺ mainly originates in this process. The weaker inhibition observed in the Mn²⁺ context is not related to a reduction of cooperativity but, most likely, to the Cys 56 modification in the central domain.

The cooperative DNA-binding of IN is related to a specific DNA-binding mode

The weaker cooperativity index for DNA binding in the presence of Mn²⁺ compared to Mg²⁺, as well as the more potent DIBA-mediated inhibition of IN catalytic activity in Mg²⁺ compared to Mn²⁺ (that originates in the DIBA-induced loss of cooperativity in Mg²⁺) confirm that the structural determinants for IN activity differ depending on the nature of the cofactor. It is well known that the Mg²⁺-dependent activity is more stringent and predictive of physiological activity than Mn²⁺-dependent activity, e.g. for resistance mutations to anti-IN compounds (45). Moreover, several functional mutations, including those in the zinc-finger motif, yield non-infectious particles and abolish Mg²⁺-dependent 3'-processing *in vitro*, whereas Mn²⁺-dependent 3'-processing and disintegration reactions are relatively insensitive to the same mutations (30,46,47). Consistent with this differential effect, it has been shown that zinc stimulates Mg²⁺-dependent, but not Mn²⁺-dependent, reaction in preparations initially depleted in zinc (48). It is then generally admitted that the zinc-finger motif does not directly mediate the catalytic process but regulates the specificity of the reaction via protein–protein interactions and facilitating IN oligomerization (27–29,49). Moreover, zinc stimulates dimerization of free monomeric IN in Mg²⁺ but not Mn²⁺ solution in the presence of detergent (27). Here, we found that the DNA binding of IN is cooperative, characterized by a Hill coefficient of 2, in agreement with previous results (18). Interestingly, this cooperativity was only observed with Mg²⁺ and significantly reduced with Mn²⁺, suggesting that Mg²⁺ and Mn²⁺ mediate distinct mechanisms of IN–DNA assembly. According to the role of the zinc finger in the multimerization process and the zinc-mediated stimulation of catalysis only in the Mg²⁺ context, we suggest a relationship between the zinc finger and the cooperative DNA-binding mode observed in the presence of Mg²⁺. Indeed, zinc ejection by DIBA-1 or deletion of the N-terminal domain, significantly decrease the Hill coefficient (Table 4). As suggested by a previous work showing that point mutations in the zinc-finger motif do not influence activity in Mn²⁺ (30), zinc

ejection by DIBA-1 should also be neutral for Mn^{2+} -dependent activity. However, the secondary binding site in the catalytic core (C56) explains why IN is inhibited by DIBA-1 in the presence of Mn^{2+} and, consequently, why the inhibitory effects of DIBA-1 do not strictly mimic the mutations in the zinc finger motif. Accordingly, the difference between IC_{50} values measured in the presence of Mg^{2+} or Mn^{2+} was even more pronounced in the context of the C56S mutation (Table 5). Therefore, the Cys 56 residue in the CC domain mainly mediates the inhibition by DIBA-1 of the full-length IN in the Mn^{2+} context (obviously, this residue fully accounts for the inhibition of CC and ΔN truncated proteins in the disintegration assay). In contrast, the inhibition of the Mg^{2+} -dependent activity is weakly or not sensitive to the C56S mutation, indicating that zinc ejection and the subsequent loss of cooperativity lead to more dramatic effects for catalysis under Mg^{2+} condition, minimizing the impact of the C56S mutation and explaining the better IN inhibition in the presence of Mg^{2+} compared to Mn^{2+} .

Taking into account that Mg^{2+} displays more reaction specificity than Mn^{2+} , our data indicate a relationship between the cooperative assembly of IN onto the DNA substrate and the reaction specificity. Indeed, Mg^{2+} -dependent DNA-binding is cooperative with the cognate U5 DNA sequence but not with random DNA sequences. Therefore, a specific conformation of IN, compatible with a cooperative DNA-binding mode, only occurs or is strongly favoured onto the cognate sequence in the presence of Mg^{2+} . Consequently, the dimeric forms responsible for 3'-processing activity (2,3,5) could have structural differences upon Mn^{2+} or Mg^{2+} binding. Alternatively, Mn^{2+} may also allow IN monomers to perform 3'-processing—hypothesis compatible with the low Hill coefficient obtained in the presence of Mn^{2+} —but complementation experiments in Mn^{2+} with individually inactive INs (49,50), as well as recent findings that monomeric IN can dimerize upon incubation with viral or random short oligonucleotides in the presence of Mn^{2+} (51), suggest that Mn^{2+} -bound IN is also active as a multimer. Consistently, we found similar long rotational correlation times, characterizing the following complexes: IN- Mg^{2+} -viral sequence, IN- Mn^{2+} -viral sequence and IN- Mg^{2+} -random sequence. All $\theta_{25^\circ\text{C}}$ values (~ 39 – 44 ns) are compatible with a dimeric HIV-1 IN bound to DNA. Altogether, our data suggest that the nature of the dimer interface or the mechanism of dimerization, but not the oligomeric status itself, is dependent on the DNA sequence and the cofactor. Regarding the influence of the DNA sequence, our data are in excellent agreement with recent results of Lesbats *et al.* (51) who also found that both viral and random sequences induce IN dimerization, but the nature of the dimer differs depending on the DNA sequence. The authors have proposed a difference in the dimeric organization of IN in terms of symmetry, with direct consequences for the tetramerization process and competency of the formed tetramer involved in the full-site integration reaction.

We have shown that the cooperative DNA-binding mode strongly depends on the cofactor context and appears to be primarily mediated by the N-terminal

domain. This however raises the question of how the nature of the cofactor bound to the central domain differentially affects structural properties of the N-terminal domain? It was previously described that cofactor binding in the catalytic core can affect by long-distance effect the conformations of both the N- and C-terminal domains (52,53). A differential effect of $\text{Mg}^{2+}/\text{Mn}^{2+}$ on such conformational changes, could explain the observed differences in the cooperative effects mediated by the N-terminal domain as a function of the cofactor context. The differential behavior of IN between the Mg^{2+} - and the Mn^{2+} -dependent catalysis, in terms of specificity (with Mg^{2+} leading to more stringent conditions for catalysis), can be explained by a different conformation or plasticity of the active site, depending on the nature of the metallic cofactor which is coordinated, in relationship with the Pearson Hard-Soft Acid-Base (HSBA) theory. Hard metal ions such as Mg^{2+} (with a small ionic radius and a d^0 electron configuration) are characterized by electron clouds which are not easily deformed, in contrast to soft metal ions such as Mn^{2+} , with a direct consequence on the dynamics of the active site or/and the nature of the IN–DNA interaction. The transmission of the long-distance effect from the CC to the N-terminal domain could be ensured by a trans HHCC–catalytic core interaction (42) and, such a transmission could be also differentially affected by the nature of the cofactor bound in the active site. From this point of view, only Mg^{2+} is compatible with cooperativity as the presence of Mn^{2+} or the absence of cofactor lead to similar low Hill coefficients (Table 4). Note that, we also observed another long-distance effect: the nature of the cofactor also influenced the ability of the C-terminal domain to affect the overall affinity of the IN–DNA complex. The apparent affinities for DNA were similar for the full-length and ΔC proteins in Mn^{2+} , but ΔC showed a lower affinity in Mg^{2+} , reinforcing the idea that the Mn^{2+} context is less stringent than Mg^{2+} . This result confirms the importance of the C-terminal domain in the correct positioning of the DNA substrate in the active site of IN, compatible with specific catalysis (54). Surprisingly, the recent X-ray structures of the PFV-1 IN in complex with a pre-processed viral DNA end, obtained in the presence of either Mg^{2+} or Mn^{2+} , do not show any metal-dependent structural difference in the organization of the active site (7), suggesting that differential effects of metal cations on the structure/dynamics of IN only occur prior to 3'-processing catalysis.

Structural relationship between the N-terminal domain of HIV-1 IN and the cooperative/specific DNA-binding mode

We found that the N-terminal domain, via the zinc-finger motif, is responsible for the cooperative DNA binding and thus plays a crucial role to form a specific IN- Mg^{2+} /DNA complex, as the cooperative DNA-binding mode strictly requires the cognate viral sequence, Mg^{2+} as a cofactor and zinc as a positive allosteric effector. What is the role of the N-terminal domain in the formation of the specific complex?

To date, it is generally admitted that the N-terminal domain of HIV-1 IN is not essential for protein–viral DNA contacts. Indeed, in the present study, we found that the deletion of the N-terminal domain was not dramatic in terms of overall affinity. Thus, the role of the N-terminal domain could be only indirect, via protein–protein interaction, consistent with the effect of zinc on the multimerization process. The nature of the protein–protein interactions involving the N-terminal domain remains to be elucidated. Based on structural data, the formation of a dimeric, 3'-processing form of IN depends primarily on the CC (persistently dimeric whatever the structure) and possibly on the N-terminal domain (7,55,56). In contrast to the C-terminal domain in the structure of the CC/C-terminal double-domain, the N-terminal domains remains dimeric in the context of the N-terminal/CC double-domain (55,56), although with a different interface compared to the isolated domain (57). In this case, the cooperative effect could be mediated by a N-terminal/N-terminal interaction. However, two recent and independent structural studies indicate that the nature of this interaction is uncertain for HIV-1(2) IN in the presence of the Lens epithelium growth factor (LEDGF/p75) (58,59), suggesting that the N-terminal/N-terminal interaction is weak and maybe not physiologically relevant. It has been previously suggested that IN oligomerization requires the interaction between the N-terminal and the CC domains, with the catalytic domain of one protomer which functions in trans with the N-terminal domain of another protomer (42), suggesting that the role of the N-terminal domain and its zinc-finger motif in the multimerization process does not necessarily imply a N-terminal/N-terminal interaction. The structure of the multimeric full-length PFV-1 IN confirms this statement (7). According to structural and biochemical data, the zinc-dependent and cooperative assembly should be then related to a *trans* N-terminal/catalytic core interaction. Interestingly, this *trans* interaction, previously evidenced by using a *N*-ethylmaleimide-modified IN (42), involves the HHCC motif and the Cys 56 residue (see below). Finally, it is important to note that a role of zinc in the dimerization process does not exclude an additional role in promoting tetramerization (28,29). Indeed, the tetrameric model (i.e. dimer of dimer) of HIV-1 IN proposed by Wang *et al.* (55) shows the zinc coordination region of the N-terminal domain of one dimer interacting with the catalytic core of the other dimer. The role of the N-terminal domain in the stabilization of the tetramer is also evidenced in the structure of the PFV-1 IN (7).

Alternatively, the Lys14 residue was recently shown by Zhao *et al.* (60) to be important for interactions with viral DNA, suggesting that the N-terminal domain could be directly involved in the assembly of the IN–viral DNA complex. Moreover, the N-terminal region that contains Lys14 is directly affected by conformational metal-induced changes (52), suggesting that this region could be crucial for establishing specific IN–viral DNA contacts and mediating the differential effects of Mg^{2+} and Mn^{2+} . Thus, it is not excluded that the HIV-1 IN N-terminal domain could play a direct and pivotal role

in the relationship between the cooperative IN assembly and the reaction specificity, by directly interacting with the viral DNA sequence. Importantly, the X-ray structure of PFV-1 IN bound to a viral DNA end highlights that the N-terminal domain is involved in interaction with DNA, together with the central and the C-terminal domains (7).

Insight into the mechanism of action of the DIBA-1 compound

DIBA-1 efficiently ejects the zinc from the N-terminal domain of IN, as shown by VIS-spectrophotometry, and efficiently inhibits IN 3'-processing activity. We found that the zinc-finger motif (HHC⁴⁰C⁴³) was a particularly important target for DIBA-1, as shown by mass spectrometry, and probably accounts for the loss of the Mg^{2+} -mediated cooperativity induced by zinc ejection. However, using truncated INs that require Mn^{2+} to mediate the disintegration reaction (11), we found that DIBA-1 could still inhibit CC and ΔN , indicating an additional effect of DIBA-1, i.e. DIBA-1 can also directly affects the catalytic site, independent of zinc ejection. Of the three Cys residues in the catalytic core, Cys 56, Cys 65 and Cys 130, mass spectrometry and site-directed mutagenesis indicated that Cys 56 was actually the DIBA-1 target. Indeed, the C65S mutant remained sensitive to DIBA-1 while C56S and C56S/C65S mutants were much less affected by DIBA-1 (this difference was only observed in the Mn^{2+} context). Altogether, our results show that the covalent binding of DIBA-1 to Cys 56 probably perturbs the integrity of the active site, as found by others with the *N*-ethylmaleimide modification (42), with a direct inhibitory effect of the catalysis. The Cys 56 residue is not essential for catalysis by itself since the C56S mutant exhibits a wild-type activity. Nevertheless, its covalent modification—which does not prevent DNA binding—probably blocks the active site into an inactive state. This effect is clearly different from the one previously observed with the modification of Cys 65 by mercaptosalicylhydrazide derivatives which efficiently inhibit IN binding to viral DNA (61). This is consistent with the location of the Cys 65 residue in the active site which is closer to the catalytic triad and the donor site compared to Cys 56.

In conclusion, DIBA-1 covalently targets both the HHCC motif in the N-terminal domain and Cys 56 in the active site. DIBA-1 binds to each target cysteine (C40, C43, C56) as a monomer (Figure 6E), consistent with the reaction mechanism proposed by by Loo *et al.* (41). Therefore, two DIBA-1 molecules are involved in the reaction with IN. Accordingly, we found that zinc ejection coincides with the reaction of two DIBA-1 molecules per IN protomer, even though only one, which targets the HHCC motif, would be sufficient for zinc ejection, the second one being trapped in the active site. It was previously suggested a *trans* interaction between the HHCC motif domain and the *N*-ethylmaleimide-sensitive site (involving Cys 56) (42). As the HHCC motif and the Cys 56 residue are both targeted by DIBA-1, some synergistic effects between the two sites could be expected regarding the overall DIBA-1-mediated

inhibition. However, the role of the Cys 56 residue in the Mg^{2+} -dependent inhibition is uncertain as DIBA-1 showed similar IC_{50} values in Mg^{2+} for the C56S, C65S and C56S/C65S mutants. Thus, the interdependency of the two mechanisms in the overall inhibition remains unclear. Taking into account that (i) the integrity of the HHCC motif is dispensable in the Mn^{2+} context and the Mn^{2+} -dependent activity is then primarily affected by the covalent modification of the Cys 56 residue, (ii) the inhibition of the Mg^{2+} -dependent activity by DIBA-1 is only slightly influenced by the mutation of the Cys 56 residue (with the zinc ejection process which fully accounts for the inhibition in Mg^{2+}), our results suggest that the relative impact of the two mechanisms of inhibition strongly depends on the cofactor initially bound to IN, and it is unlikely that these two mechanisms occur simultaneously in a given cofactor context.

Many IN inhibitors show different efficacy *in vitro* depending on the metallic cofactor used, putatively because of different chelation effects in the active site between Mg^{2+} and Mn^{2+} (61–63). Here, the extent of 3'-processing inhibition by DIBA-1 was also strongly dependent on the cofactor. The modest effect of the C56S mutation on inhibition in the Mg^{2+} compared to the Mn^{2+} context also suggests a differential chelation effect in the active site. Although we did not find significant complexation between DIBA-1 and Mn^{2+} prior to IN binding under our experimental conditions, it is not excluded that such a complexation may occur with Mn^{2+} , but not with Mg^{2+} , in the active site context for proximity reasons, based on a recent study on complexes involving bis(2-bromophenyl)disulfide and transition metals (39). However, DIBA-1 was clearly and reproducibly a better inhibitor in the context of Mg^{2+} than Mn^{2+} , suggesting that the differential effect originates mainly in the zinc ejection which can be considered as the most potent inhibition mechanism. Therefore, DIBA-1-dependent zinc ejection (this study) or the presence of a point mutation in the zinc-finger motif (30) leads to a severe catalytic defect with Mg^{2+} as a cofactor. Finally, whatever the mechanism, DIBA-1 inhibits 3'-processing although it does not perturb the overall affinity of IN for the DNA substrate. This property is clearly different than the two main anti-IN families of small molecules. INBIs inhibit 3'-processing, but competitively prevent the binding of IN to viral DNA (18). INSTIs cannot fit in the active site of the free IN and do not prevent the binding of the viral DNA (19). Instead, they selectively target the IN–viral DNA complex and, consequently, inhibit the strand transfer reaction (20). INSTIs are not or poorly efficient against 3'-processing. Here, DIBA-1 blocks catalytic 3'-processing (\neq INSTI) at a post-DNA-binding step (\neq INBI).

CONCLUSION

The overall affinities of IN for different sequences are generally similar suggesting that IN could not discern between the cognate viral DNA sequence and a random sequence at the DNA binding level. However, this study shows that

the corresponding cooperative DNA-binding properties are distinct. The factors/parameters that modulate the Hill coefficient—i.e. the nature of the DNA sequence, the nature of the metallic cofactor, the presence of zinc—probably affect IN–DNA complexes in terms of protein–protein interface or/and IN positioning on the DNA substrate, with direct consequences on the establishment of specific protein/DNA contacts rather than by changing binding free energy. DIBA-1 was discovered by a screening program (National Cancer Institute) as effective against HIV-1 and targeting retroviral NCp7 protein (31–33). Our data suggest that DIBA-1 may also targets retroviral IN. Although DIBA compounds have issues with selectivity/toxicity and bioavailability (33), our results reinforce the importance of developing anti-IN compounds with alternative non-competitive mechanisms. Compounds targeting the IN oligomerization process or acting as allosteric compounds—with different mechanisms of action compared to INBIs or INSTIs—could be effective without causing cross-resistance to INBI or INSTI compounds (64,65). Recently, peptides that modulate the IN oligomerization process were identified and called 'shiftides' (65–67). This promising approach requires a deeper understanding of the role of the different IN domains in the oligomerization process, taking into consideration the cofactor context, because it is well-established that using Mg^{2+} as a cofactor is a better predictor of anti-IN activity than using Mn^{2+} (45,68). Accordingly, the present study demonstrates that the mechanism of IN/DNA recognition significantly differs depending on the cofactor context.

FUNDING

Agence Nationale de la Recherche (06-PCVI-0015); TrioH European project (FP6 n°503480); Centre National de la Recherche Scientifique; Institut d'Alembert. Funding for open access charge: Centre National Recherche Scientifique.

Conflict of interest statement. None declared.

REFERENCES

- Delelis,O., Carayon,K., Saib,A., Deprez,E. and Mouscadet,J.F. (2008) Integrase and integration: biochemical activities of HIV-1 integrase. *Retrovirology*, **5**, 114.
- Faure,A., Calmels,C., Desjobert,C., Castroviejo,M., Caumont-Sarcos,A., Tarrago-Litvak,L., Litvak,S. and Parissi,V. (2005) HIV-1 integrase crosslinked oligomers are active *in vitro*. *Nucleic Acids Res.*, **33**, 977–986.
- Guiot,E., Carayon,K., Delelis,O., Simon,F., Tauc,P., Zubin,E., Gottikh,M., Mouscadet,J.F., Brochon,J.C. and Deprez,E. (2006) Relationship between the oligomeric status of HIV-1 integrase on DNA and enzymatic activity. *J. Biol. Chem.*, **281**, 22707–22719.
- Li,M., Mizuuchi,M., Burke,T.R. Jr and Craigie,R. (2006) Retroviral DNA integration: reaction pathway and critical intermediates. *EMBO J.*, **25**, 1295–1304.
- Delelis,O., Carayon,K., Guiot,E., Leh,H., Tauc,P., Brochon,J.C., Mouscadet,J.F. and Deprez,E. (2008) Insight into the integrase–DNA recognition mechanism. A specific DNA-binding mode revealed by an enzymatically labeled integrase. *J. Biol. Chem.*, **283**, 27838–27849.

6. Baranova, S., Tuzikov, F.V., Zakharova, O.D., Tuzikova, N.A., Calmels, C., Litvak, S., Tarrago-Litvak, L., Parissi, V. and Nevinsky, G.A. (2007) Small-angle X-ray characterization of the nucleoprotein complexes resulting from DNA-induced oligomerization of HIV-1 integrase. *Nucleic Acids Res.*, **35**, 975–987.
7. Hare, S., Shree Gupta, S., Valkov, E., Engelman, A. and Cherepanov, P. (2010) Retroviral intasome assembly and inhibition of DNA strand transfer. *Nature*, [Epub ahead of print; doi:10.1038/nature08784; 31 January 2010].
8. Chow, S.A., Vincent, K.A., Ellison, V. and Brown, P.O. (1992) Reversal of integration and DNA splicing mediated by integrase of human immunodeficiency virus. *Science*, **255**, 723–726.
9. Delelis, O., Parissi, V., Leh, H., Mbemba, G., Petit, C., Sonigo, P., Deprez, E. and Mouscadet, J.F. (2007) Efficient and specific internal cleavage of a retroviral palindromic DNA sequence by tetrameric HIV-1 integrase. *PLoS ONE*, **2**, e608.
10. Gerton, J.L. and Brown, P.O. (1997) The core domain of HIV-1 integrase recognizes key features of its DNA substrates. *J. Biol. Chem.*, **272**, 25809–25815.
11. Laboulais, C., Deprez, E., Leh, H., Mouscadet, J.F., Brochon, J.C. and Le Bret, M. (2001) HIV-1 integrase catalytic core: molecular dynamics and simulated fluorescence decays. *Biophys. J.*, **81**, 473–489.
12. Esposito, D. and Craigie, R. (1998) Sequence specificity of viral end DNA binding by HIV-1 integrase reveals critical regions for protein-DNA interaction. *EMBO J.*, **17**, 5832–5843.
13. Agapkina, J., Smolov, M., Barbe, S., Zubin, E., Zatsepin, T., Deprez, E., Le Bret, M., Mouscadet, J.F. and Gottikh, M. (2006) Probing of HIV-1 integrase/DNA interactions using novel analogs of viral DNA. *J. Biol. Chem.*, **281**, 11530–11540.
14. Skinner, L.M., Sudol, M., Harper, A.L. and Katzman, M. (2001) Nucleophile selection for the endonuclease activities of human, ovine, and avian retroviral integrases. *J. Biol. Chem.*, **276**, 114–124.
15. Engelman, A. and Craigie, R. (1995) Efficient magnesium-dependent human immunodeficiency virus type 1 integrase activity. *J. Virol.*, **69**, 5908–5911.
16. Semenova, E.A., Marchand, C. and Pommier, Y. (2008) HIV-1 integrase inhibitors: update and perspectives. *Adv. Pharmacol.*, **56**, 199–228.
17. Bonnenfant, S., Thomas, C.M., Vita, C., Subra, F., Deprez, E., Zouhiri, F., Desmaele, D., d'Angelo, J., Mouscadet, J.F. and Leh, H. (2004) Styrylquinolines, integrase inhibitors acting prior to integration: a new mechanism of action for anti-integrase agents. *J. Virol.*, **78**, 5728–5736.
18. Deprez, E., Barbe, S., Kolaski, M., Leh, H., Zouhiri, F., Auclair, C., Brochon, J.C., Le Bret, M. and Mouscadet, J.F. (2004) Mechanism of HIV-1 integrase inhibition by styrylquinoline derivatives in vitro. *Mol. Pharmacol.*, **65**, 85–98.
19. Espeseth, A.S., Felock, P., Wolfe, A., Witmer, M., Grobler, J., Anthony, N., Egbertson, M., Melamed, J.Y., Young, S., Hamill, T. et al. (2000) HIV-1 integrase inhibitors that compete with the target DNA substrate define a unique strand transfer conformation for integrase. *Proc. Natl Acad. Sci. USA*, **97**, 11244–11249.
20. Hazuda, D.J., Felock, P., Witmer, M., Wolfe, A., Stillmock, K., Grobler, J.A., Espeseth, A., Gabryelski, L., Schleif, W., Blau, C. et al. (2000) Inhibitors of strand transfer that prevent integration and inhibit HIV-1 replication in cells. *Science*, **287**, 646–650.
21. Dicker, I.B., Samanta, H.K., Li, Z., Hong, Y., Tian, Y., Banville, J., Remillard, R.R., Walker, M.A., Langley, D.R. and Krystal, M. (2007) Changes to the HIV long terminal repeat and to HIV integrase differentially impact HIV integrase assembly, activity, and the binding of strand transfer inhibitors. *J. Biol. Chem.*, **282**, 31186–31196.
22. Delelis, O., Malet, I., Na, L., Tchertanov, L., Calvez, V., Marcelin, A.G., Subra, F., Deprez, E. and Mouscadet, J.F. (2009) The G140S mutation in HIV integrases from raltegravir-resistant patients rescues catalytic defect due to the resistance Q148H mutation. *Nucleic Acids Res.*, **37**, 1193–1201.
23. Delelis, O., Thierry, S., Subra, F., Simon, F., Malet, I., Alloui, C., Sayon, S., Calvez, V., Deprez, E., Marcelin, A.G. et al. (2010) Impact of Y143 HIV-1 integrase mutations on resistance to raltegravir in vitro and in vivo. *Antimicrob. Agents Chemother.*, **54**, 491–501.
24. Yi, J., Asante-Appiah, E. and Skalka, A.M. (1999) Divalent cations stimulate preferential recognition of a viral DNA end by HIV-1 integrase. *Biochemistry*, **38**, 8458–8468.
25. Engelman, A., Hickman, A.B. and Craigie, R. (1994) The core and carboxyl-terminal domains of the integrase protein of human immunodeficiency virus type 1 each contribute to nonspecific DNA binding. *J. Virol.*, **68**, 5911–5917.
26. Gao, K., Butler, S.L. and Bushman, F. (2001) Human immunodeficiency virus type 1 integrase: arrangement of protein domains in active cDNA complexes. *EMBO J.*, **20**, 3565–3576.
27. Deprez, E., Tauc, P., Leh, H., Mouscadet, J.F., Auclair, C. and Brochon, J.C. (2000) Oligomeric states of the HIV-1 integrase as measured by time-resolved fluorescence anisotropy. *Biochemistry*, **39**, 9275–9284.
28. Zheng, R., Jenkins, T.M. and Craigie, R. (1996) Zinc folds the N-terminal domain of HIV-1 integrase, promotes multimerization, and enhances catalytic activity. *Proc. Natl Acad. Sci. USA*, **93**, 13659–13664.
29. Lee, S.P., Xiao, J., Knutson, J.R., Lewis, M.S. and Han, M.K. (1997) Zn²⁺ promotes the self-association of human immunodeficiency virus type-1 integrase in vitro. *Biochemistry*, **36**, 173–180.
30. Khan, E., Mack, J.P., Katz, R.A., Kulkosky, J. and Skalka, A.M. (1991) Retroviral integrase domains: DNA binding and the recognition of LTR sequences. *Nucleic Acids Res.*, **19**, 851–860.
31. Berthou, L., Pechoux, C. and Darlix, J.L. (1999) Multiple effects of an anti-human immunodeficiency virus nucleocapsid inhibitor on virus morphology and replication. *J. Virol.*, **73**, 10000–10009.
32. Turpin, J.A., Terpening, S.J., Schaeffer, C.A., Yu, G., Glover, C.J., Felsted, R.L., Sausville, E.A. and Rice, W.G. (1996) Inhibitors of human immunodeficiency virus type 1 zinc fingers prevent normal processing of gag precursors and result in the release of noninfectious virus particles. *J. Virol.*, **70**, 6180–6189.
33. Rice, W.G., Supko, J.G., Malspeis, L., Buckheit, R.W. Jr, Clanton, D., Bu, M., Graham, L., Schaeffer, C.A., Turpin, J.A., Domagala, J. et al. (1995) Inhibitors of HIV nucleocapsid protein zinc fingers as candidates for the treatment of AIDS. *Science*, **270**, 1194–1197.
34. Wang, L.H., Yang, X.Y., Zhang, X., Mihalic, K., Fan, Y.X., Xiao, W., Howard, O.M., Appella, E., Maynard, A.T. and Farrar, W.L. (2004) Suppression of breast cancer by chemical modulation of vulnerable zinc fingers in estrogen receptor. *Nat. Med.*, **10**, 40–47.
35. Bischerour, J., Leh, H., Deprez, E., Brochon, J.C. and Mouscadet, J.F. (2003) Disulfide-linked integrase oligomers involving C280 residues are formed in vitro and in vivo but are not essential for human immunodeficiency virus replication. *J. Virol.*, **77**, 135–141.
36. Pinskaya, M., Romanova, E., Volkov, E., Deprez, E., Leh, H., Brochon, J.C., Mouscadet, J.F. and Gottikh, M. (2004) HIV-1 integrase complexes with DNA dissociate in the presence of short oligonucleotides conjugated to acridine. *Biochemistry*, **43**, 8735–8743.
37. Hunt, J.B., Neece, S.H., Schachman, H.K. and Ginsburg, A. (1984) Mercurial-promoted Zn²⁺ release from Escherichia coli aspartate transcarbamoylase. *J. Biol. Chem.*, **259**, 14793–14803.
38. Smolov, M., Gottikh, M., Tashlitskii, V., Korolev, S., Demidyuk, I., Brochon, J.C., Mouscadet, J.F. and Deprez, E. (2006) Kinetic study of the HIV-1 DNA 3'-end processing. *FEBS J.*, **273**, 1137–1151.
39. Anaconda, J.R. and Gomez, J. (2008) Transition Metal Bis(2-Bromophenyl)disulfide complexes. *J. Chil. Chem. Soc.*, **53**, 1694–1696.
40. Zouhiri, F., Mouscadet, J.F., Mekouar, K., Desmaele, D., Savoure, D., Leh, H., Subra, F., Le Bret, M., Auclair, C. and d'Angelo, J. (2000) Structure-activity relationships and binding mode of styrylquinolines as potent inhibitors of HIV-1 integrase and replication of HIV-1 in cell culture. *J. Med. Chem.*, **43**, 1533–1540.
41. Loo, J.A., Holler, T.P., Sanchez, J., Gogliotti, R., Maloney, L. and Reily, M.D. (1996) Biophysical characterization of zinc ejection from HIV nucleocapsid protein by anti-HIV 2,2'-dithiobis[benzamides] and benzisothiazolones. *J. Med. Chem.*, **39**, 4313–4320.

42. Ellison, V., Gerton, J., Vincent, K.A. and Brown, P.O. (1995) An essential interaction between distinct domains of HIV-1 integrase mediates assembly of the active multimer. *J. Biol. Chem.*, **270**, 3320–3326.
43. Johnson, A.A., Santos, W., Pais, G.C., Marchand, C., Amin, R., Burke, T.R. Jr, Verdine, G. and Pommier, Y. (2006) Integration requires a specific interaction of the donor DNA terminal 5'-cytosine with glutamine 148 of the HIV-1 integrase flexible loop. *J. Biol. Chem.*, **281**, 461–467.
44. Johnson, A.A., Marchand, C., Patil, S.S., Costi, R., Di Santo, R., Burke, T.R. Jr and Pommier, Y. (2007) Probing HIV-1 integrase inhibitor binding sites with position-specific integrase-DNA cross-linking assays. *Mol. Pharmacol.*, **71**, 893–901.
45. Grobler, J.A., Stillmock, K., Hu, B., Witmer, M., Felock, P., Espeseth, A.S., Wolfe, A., Egbertson, M., Bourgeois, M., Melamed, J. et al. (2002) Diketo acid inhibitor mechanism and HIV-1 integrase: implications for metal binding in the active site of phosphotransferase enzymes. *Proc. Natl Acad. Sci. USA*, **99**, 6661–6666.
46. Leavitt, A.D., Robles, G., Alesandro, N. and Varmus, H.E. (1996) Human immunodeficiency virus type 1 integrase mutants retain in vitro integrase activity yet fail to integrate viral DNA efficiently during infection. *J. Virol.*, **70**, 721–728.
47. Wiskerchen, M. and Muesing, M.A. (1995) Human immunodeficiency virus type 1 integrase: effects of mutations on viral ability to integrate, direct viral gene expression from unintegrated viral DNA templates, and sustain viral propagation in primary cells. *J. Virol.*, **69**, 376–386.
48. Lee, S.P. and Han, M.K. (1996) Zinc stimulates Mg²⁺-dependent 3'-processing activity of human immunodeficiency virus type 1 integrase in vitro. *Biochemistry*, **35**, 3837–3844.
49. Yang, F., Leon, O., Greenfield, N.J. and Roth, M.J. (1999) Functional interactions of the HHCC domain of moloney murine leukemia virus integrase revealed by nonoverlapping complementation and zinc-dependent dimerization. *J. Virol.*, **73**, 1809–1817.
50. Engelman, A., Bushman, F.D. and Craigie, R. (1993) Identification of discrete functional domains of HIV-1 integrase and their organization within an active multimeric complex. *EMBO J.*, **12**, 3269–3275.
51. Lesbats, P., Metifiot, M., Calmels, C., Baranova, S., Nevinsky, G., Andreola, M.L. and Parissi, V. (2008) In vitro initial attachment of HIV-1 integrase to viral ends: control of the DNA specific interaction by the oligomerization state. *Nucleic Acids Res.*, **36**, 7043–7058.
52. Asante-Appiah, E., Seeholzer, S.H. and Skalka, A.M. (1998) Structural determinants of metal-induced conformational changes in HIV-1 integrase. *J. Biol. Chem.*, **273**, 35078–35087.
53. Asante-Appiah, E. and Skalka, A.M. (1997) A metal-induced conformational change and activation of HIV-1 integrase. *J. Biol. Chem.*, **272**, 16196–16205.
54. Ramcharan, J., Colletuori, D.M., Merkel, G., Andrade, M.D. and Skalka, A.M. (2006) Mode of inhibition of HIV-1 Integrase by a C-terminal domain-specific monoclonal antibody. *Retrovirology*, **3**, 34.
55. Wang, J.Y., Ling, H., Yang, W. and Craigie, R. (2001) Structure of a two-domain fragment of HIV-1 integrase: implications for domain organization in the intact protein. *EMBO J.*, **20**, 7333–7343.
56. Chen, J.C., Krucinski, J., Miercke, L.J., Finer-Moore, J.S., Tang, A.H., Leavitt, A.D. and Stroud, R.M. (2000) Crystal structure of the HIV-1 integrase catalytic core and C-terminal domains: a model for viral DNA binding. *Proc. Natl Acad. Sci. USA*, **97**, 8233–8238.
57. Cai, M., Zheng, R., Caffrey, M., Craigie, R., Clore, G.M. and Gronenborn, A.M. (1997) Solution structure of the N-terminal zinc binding domain of HIV-1 integrase. *Nat. Struct. Biol.*, **4**, 567–577.
58. Michel, F., Crucifix, C., Granger, F., Eiler, S., Mouscadet, J.F., Korolev, S., Agapkina, J., Ziganshin, R., Gottikh, M., Nazabal, A. et al. (2009) Structural basis for HIV-1 DNA integration in the human genome, role of the LEDGF/P75 cofactor. *EMBO J.*, **28**, 980–991.
59. Hare, S., Shun, M.C., Gupta, S.S., Valkov, E., Engelman, A. and Cherepanov, P. (2009) A novel co-crystal structure affords the design of gain-of-function lentiviral integrase mutants in the presence of modified PSIP1/LEDGF/p75. *PLoS Pathog.*, **5**, e1000259.
60. Zhao, Z., McKee, C.J., Kessler, J.J., Santos, W.L., Daigle, J.E., Engelman, A., Verdine, G. and Kvaratskhelia, M. (2008) Subunit-specific Protein Footprinting Reveals Significant Structural Rearrangements and a Role for N-terminal Lys-14 of HIV-1 Integrase during Viral DNA Binding. *J. Biol. Chem.*, **283**, 5632–5641.
61. Neamati, N., Lin, Z., Karki, R.G., Orr, A., Cowansage, K., Strumberg, D., Pais, G.C., Voigt, J.H., Nicklaus, M.C., Winslow, H.E. et al. (2002) Metal-dependent inhibition of HIV-1 integrase. *J. Med. Chem.*, **45**, 5661–5670.
62. Fesen, M.R., Pommier, Y., Leteurtre, F., Hiroguchi, S., Yung, J. and Kohn, K.W. (1994) Inhibition of HIV-1 integrase by flavones, caffeic acid phenethyl ester (CAPE) and related compounds. *Biochem. Pharmacol.*, **48**, 595–608.
63. Molteni, V., Rhodes, D., Rubins, K., Hansen, M., Bushman, F.D. and Siegel, J.S. (2000) A new class of HIV-1 integrase inhibitors: the 3,3,3', 3'-tetramethyl-1,1'-spirobi(indan)-5,5',6,6'-tetrol family. *J. Med. Chem.*, **43**, 2031–2039.
64. Serrao, E., Odde, S., Ramkumar, K. and Neamati, N. (2009) Raltegravir, elvitegravir, and metoogravir: the birth of “me-too” HIV-1 integrase inhibitors. *Retrovirology*, **6**, 25.
65. Kessler, J.J., Eidahl, J.O., Shkriabai, N., Zhao, Z., McKee, C.J., Hess, S., Burke, T.R. Jr and Kvaratskhelia, M. (2009) An allosteric mechanism for inhibiting HIV-1 integrase with a small molecule. *Mol. Pharmacol.*, **76**, 824–832.
66. Armon-Omer, A., Levin, A., Hayouka, Z., Butz, K., Hoppe-Seyler, F., Loya, S., Hizi, A., Friedler, A. and Loyter, A. (2008) Correlation between shiftase activity and HIV-1 integrase inhibition by a peptide selected from a combinatorial library. *J. Mol. Biol.*, **376**, 971–982.
67. Hayouka, Z., Rosenbluh, J., Levin, A., Loya, S., Lebendiker, M., Veprintsev, D., Kotler, M., Hizi, A., Loyter, A. and Friedler, A. (2007) Inhibiting HIV-1 integrase by shifting its oligomerization equilibrium. *Proc. Natl Acad. Sci. USA*, **104**, 8316–8321.
68. Marchand, C., Johnson, A.A., Karki, R.G., Pais, G.C., Zhang, X., Cowansage, K., Patel, T.A., Nicklaus, M.C., Burke, T.R. Jr and Pommier, Y. (2003) Metal-dependent inhibition of HIV-1 integrase by beta-diketo acids and resistance of the soluble double-mutant (F185K/C280S). *Mol. Pharmacol.*, **64**, 600–609.